Physics – Uspekhi **49** (12) 1239 – 1252 (2006)

REVIEWS OF TOPICAL PROBLEMS PACS numbers: 05.20.Dd, 52.25.Dg, **52.38. – r**

Kinetic theory of plasma and gas. Interaction of high-intensity laser pulses with plasmas

I N Kosarev

DOI: 10.1070/PU2006v049n12ABEH006027

Contents

Abstract. A kinetic theory of tenuous plasmas and gases is elaborated, which is physically equivalent to the conventional theory and is based on the construction of distribution function propagators that depend on these distribution functions. A theory of short high-intensity laser pulse – plasma interaction is constructed on the basis of this kinetic theory. A general characteristic is provided for the absorption of high-intensity laser radiation by a plasma and its associated parametric instabilities. Considered next are diverse regimes of subpicosecond relativistic laser pulse – plasma interaction. In the framework of the theory elaborated here, an investigation was made of hot-electron production in the interaction of relativistic femtosecond laser pulses with a weakly nonuniform plasma at densities of the order of and above the critical density, as well as of fast-proton production in the irradiation of a thin foil with an admixture of hydrogen. Calculations were carried out with real ion charges and at realistic ion charges and realistic plasma densities. The results are consistent both with calculations by the generally accepted particle-in-cell technique and with experimental data.

1. Introduction

The generation of short laser pulses enables obtaining high-intensity laser radiation, a high energy density, and strong magnetic fields. At present, lasers with a power of $10^{12}-10^{15}$ W exist [1, 2], making it possible to produce radiation intensities $10^{18}-10^{21}$ W cm^{-2} and megagauss magnetic fields. The characteristic duration of laser pulses is of the order of or shorter than a picosecond. When incident on a gas or solid target, such an intense laser pulse transforms it into a plasma state (plasma is also produced by a lower-intensity prepulse, which is inevitably created in the generation of the main pulse). Owing to the development of parametric instabilities, plasma waves are excited in the resultant laser-produced plasma [3 – 6]. Furthermore, with such laser radiation intensities, the ponderomotive force gives rise to a strong charge separation and, as a consequence, to quasistationary electric fields. The plasma electrons and ions are accelerated both by the plasma waves and by the quasistationary electric fields, the fields of accelerated particles having an appreciable effect on the plasma dynamics [7].

The method most extensively used in theoretical investigation of laser – plasma kinetics in this strongly nonlinear regime is the particle-in-cell technique [8], which involves a numerical solution of the Vlasov system of equations [9]. Numerically solved are the equations of motion for plasma particles in the field produced by these particles, the charge of the plasma particles being 'spread' over the cells in the coordinate space. The self-consistent plasma evolution is thereby calculated.

Proposed in this work is a different method for investigating the kinetics of tenuous plasmas and gases, which relies on the construction of a propagator for the distribution function of plasma or gas particles [10], be it a classical or a quantum plasma. This theory is outlined in Section 2. Section 3 is concerned with the theory of interaction between high-intensity laser pulses and the Coulomb plasma [11], developed on the basis of the kinetic theory of tenuous classical plasmas outlined here. Section 4 gives a brief review of the mechanisms of laser radiation absorption by a plasma and the parametric instabilities responsible for this absorption. A review of diverse relativistic subpicosecond laser pulse – plasma interaction regimes is presented in Section 5. The

I N Kosarev Russian Federal Nuclear Center — All-Russian Scientific Research Institute of Experimental Physics,
ul. Mira 37, 607190 Sarov, Nizhnii Novgorod region, Russian Federation
E-mail: kosarev@vniief.ru

Received 28 December 2005
Uspekhi Fizicheskikh Nauk **176** (12) 1267 – 1281 (2006)
Translated by E N Ragozin; edited by A M Semikhatov

new method in laser-plasma kinetics offers new opportunities in comparison with the generally accepted particle-in-cell technique: specifically, it enables investigating the plasma evolution for realistic high densities and ion charges. Dense laser plasmas with multiply charged ions may evolve in a somewhat different regime than a model plasma with a lower density and ion charge.

2. Effective action for a particle in a plasma

The conventional kinetic theory of a tenuous ($nr_{\mathrm{D}}^3 \gg 1$, where n is the particle density and r_{D} is the Debye radius) plasma is based on the system of integrodifferential equations consisting of the Boltzmann kinetic equations (for particles of each kind) with a collision integral (for instance, of the Lenard–Balescu type) and of the system of Maxwell equations with the charge and current densities expressed in terms of single-particle distribution functions, which are in turn determined from kinetic equations (see, e.g., Ref. [12]). This work presents a kinetic theory of tenuous plasmas that is physically equivalent to the conventional theory and is based on the construction of distribution function propagators dependent on these distribution functions. Therefore, investigating the plasma kinetics requires solving the system of integral equations whose number corresponds to the number of plasma particle types. This approach may be simpler than the conventional approach to the investigation of plasma kinetics.

We consider a volume V containing N_a particles of type a and N_b particles of type b. For a classical plasma, in the path integral for the particle propagator [13], it suffices to take the contribution of only the classical trajectory into account. In this case, the interaction-independent preexponential factor is calculated by solving the expansion problem for the gas of noninteracting particles. The classical propagator for the density matrix $\rho(\mathbf{r}, \mathbf{r}', t)$ is given by

$$K_a^{\mathrm{M}}(2,1) = \mu \exp\left\{\frac{\mathrm{i}}{\hbar}\left[S_a(\mathbf{r}_2, t_2; \mathbf{r}_1, t_1) - S_a(\mathbf{r}_2', t_2; \mathbf{r}_1', t_1)\right]\right\}, \qquad \mu = \left(\frac{m_a}{2\pi\hbar(t_2 - t_1)}\right)^3, \tag{1}$$

where S_a is the classical action of a particle of mass m_a:

$$S_a(\mathbf{r}_2, t_2; \mathbf{r}_1, t_1) = \int_{t_1}^{t_2} \mathrm{d}t \left\{\frac{m_a \mathbf{v}_a^2(t)}{2} - \sum_{i=2}^{N_a} U_{aa}\big(\mathbf{R}_i(t) - \mathbf{r}_a(t)\big)\right\} - \int_{t_1}^{t_2} \mathrm{d}t \left\{\sum_{j=1}^{N_b} U_{ab}\big(\mathbf{R}_j(t) - \mathbf{r}_a(t)\big) - \mathbf{F}_a(t)\mathbf{r}_a(t)\right\}. \tag{2}$$

Here, $\mathbf{v}_a(t)$ and $\mathbf{r}_a(t)$ are the velocity and the radius vector of the particle, U_{aa} and U_{ab} are the potential energies of particle interaction, $\mathbf{R}_i$ is the radius vector of the scattering center, and $\mathbf{F}_a$ is the external force acting on the particle. The particle trajectory is subject to the boundary conditions $\mathbf{r}_a(t_1) = \mathbf{r}_1$ and $\mathbf{r}_a(t_2) = \mathbf{r}_2$

The scatting centers in expressions (1) and (2) may be assumed to move along rectilinear trajectories during a time interval much shorter than the relaxation time. We first consider the plasma evolution during just these short time intervals. Propagator (1) is averaged over the ensemble with a many-particle distribution function that takes only pair correlations into account (the polarization approximation [12]):

$$f(\mathbf{R}_1, \mathbf{p}_1, \ldots, \mathbf{R}_N, \mathbf{p}_N, t) = \prod_{i=1}^{N_a+N_b} f_i(\mathbf{R}_i, \mathbf{p}_i, t) + \sum_{i \geqslant j} g(\mathbf{R}_i, \mathbf{p}_i, \mathbf{R}_j, \mathbf{p}_j, t) \prod_{k \neq i,\, j} f_k(\mathbf{R}_k, \mathbf{p}_k, t), \tag{3}$$

where $f_i(\mathbf{R}_i, \mathbf{p}_i, t)$ are single-particle distribution functions ($\mathbf{p}_i$ is the particle momentum) and $g(\mathbf{R}_i, \mathbf{p}_i, \mathbf{R}_j, \mathbf{p}_j, t)$ is the pair correlation function. The single-particle distribution functions are related to the density matrix by the equations

$$f(\mathbf{r}, \mathbf{p}, t) = \frac{V}{(2\pi\hbar)^3} \int \mathrm{d}\boldsymbol{\gamma}\, \rho\left(\mathbf{r} + \frac{\boldsymbol{\gamma}}{2}, \mathbf{r} - \frac{\boldsymbol{\gamma}}{2}, t\right) \exp\left(\mathrm{i}\,\frac{\boldsymbol{\gamma}\mathbf{p}}{\hbar}\right),$$
$$\rho(\mathbf{r}, \mathbf{r}', t) = \frac{1}{V} \int \mathrm{d}\mathbf{p}\, f\left(\mathbf{p}, \frac{\mathbf{r} + \mathbf{r}'}{2}, t\right) \exp\left(\mathrm{i}\,\frac{\mathbf{p}(\mathbf{r} - \mathbf{r}')}{\hbar}\right), \tag{4}$$
$$\int \mathrm{d}\mathbf{p} \int \frac{\mathrm{d}\mathbf{r}}{V} f(\mathbf{r}, \mathbf{p}, t) = 1, \qquad \int \mathrm{d}\mathbf{r}\, \rho(\mathbf{r}, \mathbf{r}, t) = 1.$$

Statistically averaged propagator (1) is given by

$$\begin{aligned}
K_a(2,1) &= \mu \exp\left(\frac{\mathrm{i}}{\hbar}\int_{t_1}^{t_2} \mathrm{d}t\, \frac{m_a v_a^2(t)}{2}\right) \prod_{j=1}^{N_a} \frac{1}{V} \int \mathrm{d}\mathbf{R}_j\, \mathrm{d}\mathbf{p}_j\, f_a(\mathbf{R}_j, \mathbf{p}_j, t_1) \\
&\times \exp\left[-\frac{\mathrm{i}}{\hbar}\int_{t_1}^{t_2} \mathrm{d}t\, U_{aa}\big(\mathbf{R}_j + \mathbf{v}_j(t - t_1) - \mathbf{r}_a(t)\big)\right] \\
&\times \exp\left(-\frac{\mathrm{i}}{\hbar}\int_{t_1}^{t_2} \mathrm{d}t\, \frac{m_a v_a'^2(t)}{2}\right) \prod_{j=1}^{N_a} \frac{1}{V} \int \mathrm{d}\mathbf{R}_j\, \mathrm{d}\mathbf{p}_j\, f_a(\mathbf{R}_j, \mathbf{p}_j, t_1) \\
&\times \exp\left[\frac{\mathrm{i}}{\hbar}\int_{t_1}^{t_2} \mathrm{d}t\, U_{aa}\big(\mathbf{R}_j + \mathbf{v}_j(t - t_1) - \mathbf{r}_a'(t)\big)\right] \\
&\times \prod_{j=1}^{N_b} \frac{1}{V} \int \mathrm{d}\mathbf{R}_j\, \mathrm{d}\mathbf{p}_j\, f_b(\mathbf{R}_j, \mathbf{p}_j, t_1) \\
&\times \exp\left[-\frac{\mathrm{i}}{\hbar}\int_{t_1}^{t_2} \mathrm{d}t\, U_{ba}\big(\mathbf{R}_j + \mathbf{v}_j(t - t_1) - \mathbf{r}_a(t)\big)\right] \\
&\times \prod_{j=1}^{N_b} \frac{1}{V} \int \mathrm{d}\mathbf{R}_j\, \mathrm{d}\mathbf{p}_j\, f_b(\mathbf{R}_j, \mathbf{p}_j, t_1) \\
&\times \exp\left[\frac{\mathrm{i}}{\hbar}\int_{t_1}^{t_2} \mathrm{d}t\, U_{ba}\big(\mathbf{R}_j + \mathbf{v}_j(t - t_1) - \mathbf{r}_a'(t)\big)\right] \\
&+ \sum_{cd = aa,\, bb,\, ba} \sum_{j \neq k} \int \frac{\mathrm{d}\mathbf{R}_j\, \mathrm{d}\mathbf{p}_j\, \mathrm{d}\mathbf{R}_k\, \mathrm{d}\mathbf{p}_k}{V^2}\, g_{cd}(\mathbf{R}_j, \mathbf{p}_j, \mathbf{R}_k, \mathbf{p}_k, t_1) \\
&\times \exp\left[\frac{\mathrm{i}}{\hbar}\int_{t_1}^{t_2} \mathrm{d}t \left(\frac{m_a v_a^2(t)}{2} - U_{cd}\big(\mathbf{R}_j + \mathbf{v}_j(t - t_1) - \mathbf{r}_a(t)\big)\right)\right] \\
&\times \exp\left[-\frac{\mathrm{i}}{\hbar}\int_{t_1}^{t_2} \mathrm{d}t \left(\frac{m_a v_a'^2(t)}{2} - U_{cd}\big(\mathbf{R}_j + \mathbf{v}_j(t - t_1) - \mathbf{r}_a'(t)\big)\right)\right] \\
&\times \prod_{l \neq j,\, k} \frac{1}{V} \int \mathrm{d}\mathbf{R}_l\, \mathrm{d}\mathbf{p}_l\, f_a(\mathbf{R}_l, \mathbf{p}_l, t_1) \\
&\times \exp\left[-\frac{\mathrm{i}}{\hbar}\int_{t_1}^{t_2} \mathrm{d}t\, U_{aa}\big(\mathbf{R}_l + \mathbf{v}_l(t - t_1) - \mathbf{r}_a(t)\big)\right] \\
&\times \exp\left[\frac{\mathrm{i}}{\hbar}\int_{t_1}^{t_2} \mathrm{d}t\, U_{aa}\big(\mathbf{R}_l + \mathbf{v}_l(t - t_1) - \mathbf{r}_a'(t)\big)\right]
\end{aligned}$$

$$\times \prod_{l\neq j,k} \frac{1}{V}\int \mathrm{d}\mathbf{R}_l\,\mathrm{d}\mathbf{p}_l\, f_b(\mathbf{R}_l,\mathbf{p}_l,t_1)$$
$$\times \exp\left[-\frac{\mathrm{i}}{\hbar}\int_{t_1}^{t_2}\mathrm{d}t\, U_{ba}\big(\mathbf{R}_l+\mathbf{v}_l(t-t_1)-\mathbf{r}_a(t)\big)\right]$$
$$\times \exp\left[\frac{\mathrm{i}}{\hbar}\int_{t_1}^{t_2}\mathrm{d}t\, U_{ba}\big(\mathbf{R}_l+\mathbf{v}_l(t-t_1)-\mathbf{r}'_a(t)\big)\right], \qquad (5)$$

where the averaging is performed with the one- and two-particle distribution functions. The subsequent transformations are similar to those used in constructing the adiabatic broadening theory [14]. We first make the identical transformation

$$\prod_{j=1}^{N}\int \frac{\mathrm{d}\mathbf{R}}{V}\,\mathrm{d}\mathbf{p}\, f(\mathbf{R},\mathbf{p},t)$$
$$\times \exp\left[\frac{\mathrm{i}}{\hbar}\int_{t_1}^{t_2}\mathrm{d}t\, U\big(\mathbf{R}+\mathbf{v}(t-t_1)-\mathbf{r}(t)\big)\right]$$
$$= \prod_{j=1}^{N}\int \frac{\mathrm{d}\mathbf{R}}{V}\,\mathrm{d}\mathbf{p}\, f(\mathbf{R},\mathbf{p},t)$$
$$\times \left\{1+\exp\left[\frac{\mathrm{i}}{\hbar}\int_{t_1}^{t_2}\mathrm{d}t\, U\big(\mathbf{R}+\mathbf{v}(t-t_1)-\mathbf{r}(t)\big)\right]-1\right\}. \qquad (6)$$

In the limit $N\to\infty$, $V\to\infty$ and in view of the definition of $\mathrm{e}=\lim_{N\to\infty}(1+1/N)^N$, expression (6) can be written as

$$\prod_{j=1}^{N}\int \frac{\mathrm{d}\mathbf{R}}{V}\,\mathrm{d}\mathbf{p}\, f(\mathbf{R},\mathbf{p},t)$$
$$\times \exp\left[\frac{\mathrm{i}}{\hbar}\int_{t_1}^{t_2}\mathrm{d}t\, U\big(\mathbf{R}+\mathbf{v}(t-t_1)-\mathbf{r}(t)\big)\right]$$
$$= \exp\left\{n\int \mathrm{d}\mathbf{R}\,\mathrm{d}\mathbf{p}\, f(\mathbf{R},\mathbf{p},t)\right.$$
$$\left.\times\left[\exp\left(\frac{\mathrm{i}}{\hbar}\int_{t_1}^{t_2}\mathrm{d}t\, U\big(\mathbf{R}+\mathbf{v}(t-t_1)-\mathbf{r}(t)\big)\right)-1\right]\right\}, \qquad (7)$$

where $n=N/V$.

With expressions (6) and (7), transformation (5) leads to the propagator with an effective action. The averaged propagator is given by

$$K_a(2,1)$$
$$= \mu\exp\left\{\frac{\mathrm{i}}{\hbar}\int_{t_1}^{t_2}\mathrm{d}t\left(\frac{m_a\mathbf{v}_a^2(t)}{2}-\frac{m_a\mathbf{v}_a'^2(t)}{2}\right)+n_aV_{aa}^{\mathrm{st}}+n_bV_{ba}^{\mathrm{st}}\right\}$$
$$\times\exp\left\{\frac{\mathrm{i}}{\hbar}\int_{t_1}^{t_2}\mathrm{d}t\left[\mathbf{F}_a(t)\mathbf{r}_a(t)-\mathbf{F}_a(t)\mathbf{r}'_a(t)\right]\right\}$$
$$+\mu\sum_{ij=aa,ba,bb}\frac{n_in_j}{2}\int \mathrm{d}\mathbf{R}_1\,\mathrm{d}\mathbf{R}_2\,\mathrm{d}\mathbf{p}_1\,\mathrm{d}\mathbf{p}_2\, g_{ij}(\mathbf{R}_1,\mathbf{p}_1,\mathbf{R}_2,\mathbf{p}_2,t_1)$$
$$\times\exp\left\{\frac{\mathrm{i}}{\hbar}\int_{t_1}^{t_2}\mathrm{d}t\sum_{k=1,2}-U_{ij}\big(\mathbf{R}_k-\mathbf{v}_k(t_2-t)-\mathbf{r}_{a,ij}(t)\big)\right\}$$
$$\times\exp\left\{\frac{\mathrm{i}}{\hbar}\int_{t_1}^{t_2}\mathrm{d}t\sum_{k=1,2}U_{ij}\big(\mathbf{R}_k-\mathbf{v}_k(t_2-t)-\mathbf{r}'_{a,ij}(t)\big)\right\}$$
$$\times\exp\left\{\frac{\mathrm{i}}{\hbar}\int_{t_1}^{t_2}\mathrm{d}t\left(\frac{m_a\mathbf{v}_{a,ij}^2(t)}{2}-\frac{m_a\mathbf{v}_{a,ij}'^2(t)}{2}\right)+n_aV_{aa}^{\mathrm{st}}+n_bV_{ba}^{\mathrm{st}}\right\}$$
$$\times\exp\left\{\frac{\mathrm{i}}{\hbar}\int_{t_1}^{t_2}\mathrm{d}t\left[\mathbf{F}_a(t)\mathbf{r}_{a,ij}(t)-\mathbf{F}_a(t)\mathbf{r}'_{a,ij}(t)\right]\right\}, \qquad (8)$$

where $g_{ba}(\mathbf{R}_1,\mathbf{p}_1,\mathbf{R}_2,\mathbf{p}_2,t)$ is the pair correlation function, which is expressed in terms of the single-particle distribution functions $f_{a,b}(\mathbf{r},\mathbf{p},t)$ [12], and V_{ba}^{st} is the collision volume (see the adiabatic broadening theory [14]):

$$V_{ba}^{\mathrm{st}} = \int \mathrm{d}\mathbf{p}\,\mathrm{d}\mathbf{R}\, f_b(\mathbf{R},\mathbf{p},t_1)$$
$$\times\left[\exp\left\{-\frac{\mathrm{i}}{\hbar}\int_{t_1}^{t_2}\mathrm{d}t\left[U_{ba}\big(\mathbf{R}-\mathbf{v}(t_2-t)-\mathbf{r}_a(t)\big)\right.\right.\right.$$
$$\left.\left.\left.-U_{ba}\big(\mathbf{R}-\mathbf{v}(t_2-t)-\mathbf{r}'_a(t)\big)\right]\right\}-1\right]. \qquad (9)$$

The first term in propagator (8) determines the evolution of the distribution function in the self-consistent field approximation and the term with the collision volume (9) (in the exponent) determines the plasma particle deceleration (acceleration) by the self-consistent field. The subsequent terms describe the effect of collisions on the plasma kinetics.

For the Coulomb interaction, estimating the Weisskopf radius yields a value of the order of the minimal impact parameter $r_{\min}$ in the Landau collision integral [9]. The averaged effect of the fields of the scattering centers on the particle trajectories in expression (8) may be taken into account using the perturbation theory in the small parameters $U(r_{\mathrm{D}})/U(r_{\min})$ and $nr_{\min}^3$, where r_{D} is the Debye radius, which determines the characteristic correlation length for plasma particles. Hence, the terms in the effective action with a complicated dependence on the trajectory may be taken into account using the perturbation theory, and the effective action may therefore be calculated analytically in many cases. This is done for the laser pulse–plasma interaction below.

The propagator in (8) and (9) describes the plasma dynamics for short time intervals, shorter than the distribution function relaxation time. If the plasma density matrix is known at a time instant t_1, then at t_2 it is given by the relation

$$\rho_a(\mathbf{r}_2,\mathbf{r}'_2,t_2)=\int \mathrm{d}\mathbf{r}_1\int \mathrm{d}\mathbf{r}'_1\, K_a(2,1)\,\rho_a(\mathbf{r}_1,\mathbf{r}'_1,t_1)\,. \qquad (10)$$

When the external force is so strong that $Fr_{\min}\geqslant U(r_{\min})$, the effect of this force on the correlation functions must be taken into account [12].

For a relativistic plasma, the relativistic expression for the kinetic energy of a particle is to be substituted in Eqn (2) and not only the scalar potential of the scattering centers but also the vector potential must be taken into account [15].

In a quantum plasma, when calculating the path integral for the propagator, it is necessary to include the contribution not only of the classical trajectory but also of all the other ones. Statistical averaging is performed with the many-particle density matrix taking only pair correlations into account:

$$\rho_N(\mathbf{R}_1,\mathbf{R}'_1,\ldots,\mathbf{R}_N,\mathbf{R}'_N,t)=\prod_{j=1}^{N}\rho(\mathbf{R}_j,\mathbf{R}'_j,t)$$
$$+\sum_{j>k}g(\mathbf{R}_j,\mathbf{R}'_j,\mathbf{R}_k,\mathbf{R}'_k,t)\prod_{l\neq j,k}\rho(\mathbf{R}_l,\mathbf{R}'_l,t)\,,$$
$$\int\frac{\mathrm{d}\mathbf{R}_j}{V}\,\rho(\mathbf{R}_j,\mathbf{R}_j,t)=1\,. \qquad (11)$$

In the polarization approximation, the quantum correlation function is expressed in terms of single-particle density matrices (see part 3 of monograph [12] and the references

therein). The exchange interaction is included in the quantum correlation function.

In the case of a quantum plasma, the propagator

$$K_a^{\mathrm{M}}(2,1) = \int D\big[\mathbf{r}_a(t)\big] \int D\big[\mathbf{r}'_a(t)\big] \times \prod_{j=1}^{N_a+N_b} \int_{\mathbf{R}_j(t_1)=\mathbf{R}_{j1}}^{\mathbf{R}_j(t_2)=\mathbf{R}_{j2}} D\big[\mathbf{R}_j(t)\big] \exp\left[\frac{\mathrm{i}}{\hbar}\int_{t_1}^{t_2} \mathrm{d}t\, \frac{M_j\dot{\mathbf{R}}_j^2(t)}{2}\right] \times \exp\left\{\frac{\mathrm{i}}{\hbar}\big[S_a(\mathbf{r}_2,t_2;\mathbf{r}_1,t_1) - S_a(\mathbf{r}'_2,t_2;\mathbf{r}'_1,t_1)\big]\right\} \tag{12}$$

must be averaged with (11) and with the action S_a in expression (2). Propagator (12) has the meaning of the conditional transition probability for a test particle. After transformations similar to (6) and (7), we obtain the expression for the averaged propagator as

$$\begin{aligned} K_a(2,1) &= \int D\big[\mathbf{r}_a(t)\big] \int D\big[\mathbf{r}'_a(t)\big] \\ &\times \exp\left\{\frac{\mathrm{i}}{\hbar}\int_{t_1}^{t_2} \mathrm{d}t \left[\frac{m_a\mathbf{v}_a^2(t)}{2} - \frac{m_a\mathbf{v}_a'^2(t)}{2}\right]\right\} \\ &\times \exp\left\{\frac{\mathrm{i}}{\hbar}\int_{t_1}^{t_2} \mathrm{d}t \left[\mathbf{F}_a(t)\mathbf{r}_a(t) - \mathbf{F}_a(t)\mathbf{r}'_a(t)\right] + n_a V_{aa}^{\mathrm{st}} + n_b V_{ba}^{\mathrm{st}}\right\} \\ &+ \sum_{ij=aa,ba,bb} \frac{n_i n_j}{2} \int \mathrm{d}\mathbf{R}_1\, \mathrm{d}\mathbf{R}_2\, \mathrm{d}\mathbf{R}'_1\, \mathrm{d}\mathbf{R}'_2 \\ &\times \big[g_{ij}(\mathbf{R}_1,\mathbf{R}_1,\mathbf{R}_2,\mathbf{R}_2,t_1)\, \rho_i(\mathbf{R}'_1,\mathbf{R}'_1,t_1)\, \rho_j(\mathbf{R}'_2,\mathbf{R}'_2,t_1) \\ &+ g_{ij}(\mathbf{R}'_1,\mathbf{R}'_1,\mathbf{R}'_2,\mathbf{R}'_2,t_1)\, \rho_i(\mathbf{R}_1,\mathbf{R}_1,t_1)\, \rho_j(\mathbf{R}_2,\mathbf{R}_2,t_1)\big] \\ &\times \int D\big[\mathbf{r}_a(t)\big] \int D\big[\mathbf{r}'_a(t)\big] \\ &\times \int_{\mathbf{R}_1(t_1)=\mathbf{R}'_1}^{\mathbf{R}_1(t_2)=\mathbf{R}_1} D\big[\mathbf{R}_1(t)\big] \int_{\mathbf{R}_2(t_1)=\mathbf{R}'_2}^{\mathbf{R}_2(t_2)=\mathbf{R}_2} D\big[\mathbf{R}_2(t)\big] \\ &\times \exp\left\{\frac{\mathrm{i}}{\hbar}\int_{t_1}^{t_2} \mathrm{d}t \sum_{k=1,2}\left[\frac{m_k\dot{\mathbf{R}}_k^2(t)}{2} - U_{ij}\big(\mathbf{R}_k(t) - \mathbf{r}_a(t)\big)\right]\right\} \\ &\times \exp\left\{\frac{\mathrm{i}}{\hbar}\int_{t_1}^{t_2} \mathrm{d}t \sum_{k=1,2} U_{ij}\big(\mathbf{R}_k(t) - \mathbf{r}'_a(t)\big)\right\} \\ &\times \exp\left\{\frac{\mathrm{i}}{\hbar}\int_{t_1}^{t_2} \mathrm{d}t \left[\frac{m_a\mathbf{v}_a^2(t)}{2} - \frac{m_a\mathbf{v}_a'^2(t)}{2}\right] + n_a V_{aa}^{\mathrm{st}} + n_b V_{ba}^{\mathrm{st}}\right\} \\ &\times \exp\left\{\frac{\mathrm{i}}{\hbar}\int_{t_1}^{t_2} \mathrm{d}t \left[\mathbf{F}_a(t)\mathbf{r}_a(t) - \mathbf{F}_a(t)\mathbf{r}'_a(t)\right]\right\}, \end{aligned} \tag{13}$$

where the collision volume is given by

$$V_{ba}^{\mathrm{st}} = \int \mathrm{d}\mathbf{R}'\, \mathrm{d}\mathbf{R}\, \rho_b(\mathbf{R},\mathbf{R},t_1)\, \rho_a(\mathbf{R}',\mathbf{R}',t_1) \int_{\mathbf{R}(t_1)=\mathbf{R}'}^{\mathbf{R}(t_2)=\mathbf{R}} D\big[\mathbf{R}(t)\big] \times \left[\exp\left\{-\frac{\mathrm{i}}{\hbar}\int_{t_1}^{t_2} \mathrm{d}t \left[\frac{m_b\dot{\mathbf{R}}^2(t)}{2} + U_{ba}\big(\mathbf{R}(t) - \mathbf{r}_a(t)\big) - U_{ba}\big(\mathbf{R}(t) - \mathbf{r}'_a(t)\big)\right]\right\} - 1\right]. \tag{14}$$

In a tenuous plasma, the perturbation theory can be used to calculate the path integrals for scattering particles in expressions (13) and (14) [13]; it then suffices to restrict ourself to the zeroth order (quantum free motion). In other words, the operation of integrating over the trajectories of perturbing particles amounts to

$$\begin{aligned} &\int_{\mathbf{R}(t_1)=\mathbf{R}_1}^{\mathbf{R}(t_2)=\mathbf{R}_2} D\big[\mathbf{R}(t)\big] \exp\left(\frac{\pm\mathrm{i}}{\hbar}\int_{t_1}^{t_2} \mathrm{d}t\, \frac{M\dot{\mathbf{R}}^2(t)}{2}\right) F\big[\mathbf{R}(t)\big] \\ &\quad\to \left[\frac{2\pi(\pm\mathrm{i})\,\hbar(t_2-t_1)}{M}\right]^{-3/2} \exp\left(\frac{\pm\mathrm{i}M(\mathbf{R}_2-\mathbf{R}_1)^2}{2\hbar(t_2-t_1)}\right) \\ &\quad\times F\left[\mathbf{R}_1 + \frac{\mathbf{R}_2-\mathbf{R}_1}{t_2-t_1}(t-t_1)\right]. \end{aligned} \tag{15}$$

Similarly to the above case of a classical plasma, the averaged effect of perturbing particles on a test particle can also be incorporated using the perturbation theory (the characteristic velocities of the quantum plasma component are of the order of the Fermi velocity). Therefore, the propagator in (13) and (14) can be analytically calculated whenever an analytic expression for the propagator of a single particle in an external field can be found.

Using the propagators with the effective actions obtained above, it is also possible to investigate the kinetics of tenuous gases. In this case, the corresponding short-range potential interaction energies for gas particles $U(\mathbf{R})$ and the Boltzmann correlation function $g(\mathbf{R}_1,\mathbf{p}_1,\mathbf{R}_2,\mathbf{p}_2,t)$ should be used [12].

In some cases, when higher-order correlation functions are insignificant, the above kinetic theory is also valid for dense plasmas and gases: for a sufficiently short time interval, the perturbation theory is again appropriate for taking the collision volume into account. In this case, pair correlation functions for dense plasmas and gases must also be used.

In a tenuous plasma, it is also possible to construct the propagator for the distribution function for longer times, i.e., those exceeding the relaxation time in the plasma. For this, the time interval is divided into short intervals that are shorter than the relaxation time but longer than the correlation decoupling times [12]. Statistical averaging is performed over the product of many-particle distribution functions (3) taken at different time instants. In view of the smallness of the correlation functions in a tenuous plasma, the averaged propagator is given by

$$\begin{aligned} &\frac{1}{\mu}\, K_a(2,1) \\ &= \exp\left\{\frac{\mathrm{i}}{\hbar}\int_{t_1}^{t_2} \mathrm{d}t \left[\frac{m_a\mathbf{v}_a^2(t)}{2} - \frac{m_a\mathbf{v}_a'^2(t)}{2}\right] + n_a V_{aa}^{\mathrm{st}} + n_b V_{ba}^{\mathrm{st}}\right\} \\ &\times \exp\left\{\frac{\mathrm{i}}{\hbar}\int_{t_1}^{t_2} \mathrm{d}t \big[\mathbf{F}_a(t)\mathbf{r}_a(t) - \mathbf{F}_a(t)\mathbf{r}'_a(t)\big]\right\} \\ &+ \sum_{ij=aa,ba,bb} \frac{n_i n_j}{2} \int \mathrm{d}\mathbf{R}_1\, \mathrm{d}\mathbf{R}_2\, \mathrm{d}\mathbf{p}_1\, \mathrm{d}\mathbf{p}_2 \int_{t_1}^{t_2} g_{ij}(\mathbf{R}_1,\mathbf{p}_1,\mathbf{R}_2,\mathbf{p}_2,t_f) \\ &\times \exp\left\{\frac{\mathrm{i}}{\hbar}\int_{t_f-\mathrm{d}t_f}^{t_f} \mathrm{d}t \sum_{k=1,2} -U_{ij}\big(\mathbf{R}_k - \mathbf{v}_k(t_2-t) - \mathbf{r}_{a,ij}(t)\big)\right\} \\ &\times \exp\left\{\frac{\mathrm{i}}{\hbar}\int_{t_f-\mathrm{d}t_f}^{t_f} \mathrm{d}t \sum_{k=1,2} U_{ij}\big(\mathbf{R}_k - \mathbf{v}_k(t_2-t) - \mathbf{r}'_{a,ij}(t)\big)\right\} \\ &\times \exp\left\{\frac{\mathrm{i}}{\hbar}\int_{t_f-\mathrm{d}t_f}^{t_f} \mathrm{d}t \left[\frac{m_a\mathbf{v}_{a,ij}^2(t)}{2} - \frac{m_a\mathbf{v}_{a,ij}'^2(t)}{2}\right] \right. \\ &\left. + n_a V_{aa}^{\mathrm{st}} + n_b V_{ba}^{\mathrm{st}}\right\} \\ &\times \exp\left\{\frac{\mathrm{i}}{\hbar}\int_{t_f-\mathrm{d}t_f}^{t_f} \mathrm{d}t \big[\mathbf{F}_a(t)\mathbf{r}_{a,ij}(t) - \mathbf{F}_a(t)\mathbf{r}'_{a,ij}(t)\big]\right\}, \end{aligned} \tag{16}$$

where

$$V_{ba}^{\mathrm{st}} = \int \mathrm{d}\mathbf{p}\,\mathrm{d}\mathbf{R} \int_{t_1}^{t_2} f_b(\mathbf{R},\mathbf{p},t_f) \times \left[\exp\left\{-\frac{\mathrm{i}}{\hbar}\int_{t_f-\mathrm{d}t_f}^{t_f} \mathrm{d}t\left[U_{ba}\big(\mathbf{R}-\mathbf{v}(t_2-t)-\mathbf{r}_a(t)\big) - U_{ba}\big(\mathbf{R}-\mathbf{v}(t_2-t)-\mathbf{r}'_a(t)\big)\right]\right\}-1\right] \tag{17}$$

is the collision volume. In formulas (16) and (17), $\mathrm{d}t_f$ is a physically infinitely short time interval, which is shorter than the relaxation time and longer than the correlation time for particles in the plasma.

For a quantum system, the averaged propagator is written as

$$\begin{aligned}
K_a(2,1) &= \int D\big[\mathbf{r}_a(t)\big]\int D\big[\mathbf{r}'_a(t)\big] \\
&\times \exp\left\{\frac{\mathrm{i}}{\hbar}\int_{t_1}^{t_2}\mathrm{d}t\left[\frac{m_a\mathbf{v}_a^2(t)}{2}-\frac{m_a\mathbf{v}_a'^2(t)}{2}\right]\right\} \\
&\times \exp\left\{\frac{\mathrm{i}}{\hbar}\int_{t_1}^{t_2}\mathrm{d}t\left[\mathbf{F}_a(t)\mathbf{r}_a(t)-\mathbf{F}_a(t)\mathbf{r}'_a(t)\right]+n_aV_{aa}^{\mathrm{st}}+n_bV_{ba}^{\mathrm{st}}\right\} \\
&+ \sum_{ij=aa,ba,bb}\frac{n_in_j}{2}\int \mathrm{d}\mathbf{R}_1\,\mathrm{d}\mathbf{R}_2\,\mathrm{d}\mathbf{R}'_1\,\mathrm{d}\mathbf{R}'_2 \\
&\times \int_{t_1}^{t_2}\big[g_{ij}(\mathbf{R}_1,\mathbf{R}_1,\mathbf{R}_2,\mathbf{R}_2,t_f)\,\rho_i(\mathbf{R}'_1,\mathbf{R}'_1,t_f)\,\rho_j(\mathbf{R}'_2,\mathbf{R}'_2,t_f) \\
&+ g_{ij}(\mathbf{R}'_1,\mathbf{R}'_1,\mathbf{R}'_2,\mathbf{R}'_2,t_f)\,\rho_i(\mathbf{R}_1,\mathbf{R}_1,t_f)\,\rho_j(\mathbf{R}_2,\mathbf{R}_2,t_f)\big] \\
&\times \int D\big[\mathbf{r}_a(t)\big]\int D\big[\mathbf{r}'_a(t)\big] \\
&\times \int_{\mathbf{R}_1(t_f-\mathrm{d}t_f)=\mathbf{R}'_1}^{\mathbf{R}_1(t_f)=\mathbf{R}_1} D\big[\mathbf{R}_1(t)\big]\int_{\mathbf{R}_2(t_f-\mathrm{d}t_f)=\mathbf{R}'_2}^{\mathbf{R}_2(t_f)=\mathbf{R}_2} D\big[\mathbf{R}_2(t)\big] \\
&\times \exp\left\{\frac{\mathrm{i}}{\hbar}\int_{t_f-\mathrm{d}t_f}^{t_f}\mathrm{d}t\sum_{k=1,2}\left[\frac{m_k\dot{\mathbf{R}}_k^2(t)}{2}-U_{ij}\big(\mathbf{R}_k(t)-\mathbf{r}_a(t)\big)\right]\right\} \\
&\times \exp\left\{\frac{\mathrm{i}}{\hbar}\int_{t_f-\mathrm{d}t_f}^{t_f}\mathrm{d}t\sum_{k=1,2}U_{ij}\big(\mathbf{R}_k(t)-\mathbf{r}'_a(t)\big)\right\} \\
&\times \exp\left\{\frac{\mathrm{i}}{\hbar}\int_{t_f-\mathrm{d}t_f}^{t_f}\mathrm{d}t\left[\frac{m_a\mathbf{v}_a^2(t)}{2}-\frac{m_a\mathbf{v}_a'^2(t)}{2}\right]+n_aV_{aa}^{\mathrm{st}}+n_bV_{ba}^{\mathrm{st}}\right\} \\
&\times \exp\left\{\frac{\mathrm{i}}{\hbar}\int_{t_f-\mathrm{d}t_f}^{t_f}\mathrm{d}t\left[\mathbf{F}_a(t)\mathbf{r}_a(t)-\mathbf{F}_a(t)\mathbf{r}'_a(t)\right]\right\},
\end{aligned} \tag{18}$$

where the collision volume is

$$V_{ba}^{\mathrm{st}} = \int \mathrm{d}\mathbf{R}'\,\mathrm{d}\mathbf{R}\int_{t_1}^{t_2}\rho_b(\mathbf{R},\mathbf{R},t_f)\,\rho_a(\mathbf{R}',\mathbf{R}',t_f) \times \int_{\mathbf{R}(t_f-\mathrm{d}t_f)=\mathbf{R}'}^{\mathbf{R}(t_f)=\mathbf{R}} D\big[\mathbf{R}(t)\big] \times \left[\exp\left\{-\frac{\mathrm{i}}{\hbar}\int_{t_f-\mathrm{d}t_f}^{t_f}\mathrm{d}t\left[\frac{m_b\dot{\mathbf{R}}^2(t)}{2}+U_{ba}\big(\mathbf{R}(t)-\mathbf{r}_a(t)\big) - U_{ba}\big(\mathbf{R}(t)-\mathbf{r}'_a(t)\big)\right]\right\}-1\right]. \tag{19}$$

Thus, we have obtained propagators (16)–(19) for a tenuous plasma, which may be calculated analytically in the majority of cases. Their application to the initial distribution function according to expression (10) leads [in view of relations (4)] to formulating the kinetic theory in the form of a system of integral equations. The evolution of a tenuous plasma may also be investigated by multiple application of propagators (8), (9) and (10), (14) if the time intervals considered are shorter than the relaxation time.

3. Kinetic theory of high-intensity short laser pulse – plasma interactions

In what follows, we use the propagator derived above for the plasma distribution function for short times (shorter than the plasma relaxation time). The idea is to investigate the plasma kinetics over sufficiently long times by multiple successive application of the propagator in accordance with relation (10). For a classical nondegenerate plasma consisting of particles of two sorts a and b, the propagator for the density matrix $\rho_a(\mathbf{r},\mathbf{r}',t)$ is given by (in the self-consistent field approximation)

$$\begin{aligned}
K_a(2,1) &= \\
&= \exp\left\{\frac{\mathrm{i}}{\hbar}\int_{t_1}^{t_2}\mathrm{d}t\left[-m_ac^2\sqrt{1-\frac{\mathbf{v}_a^2(t)}{c^2}}+m_ac^2\sqrt{1-\frac{\mathbf{v}_a'^2(t)}{c^2}}\right] + n_aV_{aa}^{\mathrm{st}}+n_bV_{ba}^{\mathrm{st}}\right\} \\
&\times \exp\left\{\frac{\mathrm{i}}{\hbar}\int_{t_1}^{t_2}\mathrm{d}t\left[\frac{Z_ae}{c}\,\mathbf{A}(t)\mathbf{v}_a(t)-\frac{Z_ae}{c}\,\mathbf{A}(t)\mathbf{v}'_a(t)\right]\right\} \\
&\times \left(\frac{m_a}{2\pi\hbar(t_2-t_1)}\right)^3,
\end{aligned} \tag{20}$$

$$V_{ba}^{\mathrm{st}} = \int \mathrm{d}\mathbf{p}\,\mathrm{d}\mathbf{R}\,f_b(\mathbf{R},\mathbf{p},t_1) \times \left[\exp\left\{-\frac{\mathrm{i}}{\hbar}\int_{t_1}^{t_2}\mathrm{d}t\left[U_{ba}\big(\mathbf{R}-\mathbf{v}(t_2-t)-\mathbf{r}_a(t)\big) - U_{ba}\big(\mathbf{R}-\mathbf{v}(t_2-t)-\mathbf{r}'_a(t)\big)\right]\right\}-1\right],$$

where $\mathbf{v}_a$ and $\mathbf{r}_a$ are the velocity and the radius vector of particle a, U_{aa} and U_{ba} are the potential energies of particle interaction, $\mathbf{R}_i$ is the radius vector of the scattering center, $\mathbf{A}$ is the vector potential of the external field acting on the particle, and n_a and Z_a are the average density and charge of the particles of sort a. Propagator (20) describes the plasma dynamics for short times, shorter than the distribution-function relaxation time. If the plasma density matrix is known at a time t_1, then its value at t_2 is defined by relation (10).

In the analysis of plasma kinetics, we can conveniently go over to the difference variable $\Delta\mathbf{r}=\mathbf{R}-\mathbf{R}'$, $\mathbf{r}=(\mathbf{R}+\mathbf{R}')/2$, $\rho(\mathbf{r}+\Delta\mathbf{r}/2,\mathbf{r}-\Delta\mathbf{r}/2)$. This density matrix is related to the distribution function by the equation

$$\begin{aligned}
f(\mathbf{r},\mathbf{p}) &= \frac{V}{(2\pi\hbar)^3}\int \mathrm{d}\Delta\mathbf{r}\,\rho(\mathbf{r},\Delta\mathbf{r})\exp\left(-\mathrm{i}\,\frac{\Delta\mathbf{r}\cdot\mathbf{p}}{\hbar}\right), \\
\rho(\mathbf{r},\Delta\mathbf{r}) &= \frac{1}{V}\int \mathrm{d}\mathbf{p}\,f(\mathbf{r},\mathbf{p})\exp\left(\mathrm{i}\,\frac{\Delta\mathbf{r}\cdot\mathbf{p}}{\hbar}\right),
\end{aligned} \tag{21}$$

where V is the plasma volume.

Because quantum effects are unessential in the problem under investigation, the particle action

$$S_a\bigl[\mathbf{r}(t),\Delta\mathbf{r}(t)\bigr]=\frac{\hbar}{\mathrm{i}}\ln\left(\frac{m_a}{2\pi\hbar(t_2-t_1)}\right)^{-3}K_a(2,1)$$

[see expression (20)] can be expanded in small $\Delta\mathbf{r}(t)$. Since the zeroth-order contribution vanishes, this expansion is equivalent to passing to the nonrelativistic limit. The nonrelativistic expression can be used for the action; the relation between the velocity and the momentum remains relativistic as in the conventional kinetic theory (in the self-consistent field approximation) [12]. In the self-consistent field approximation, for the propagator for classical-plasma particles of sort a, we obtain the expression

$$K_a(2,1)=\left(\frac{m_a}{2\pi\hbar(t_2-t_1)}\right)^3\exp\left[\frac{\mathrm{i}}{\hbar}(S_0+\Delta S_\mathrm{p})+\Delta S_\mathrm{st}\right], \quad (22)$$

where S_0 is the action of a particle in a linearly polarized laser field (typical for high-intensity lasers), in which the field nonuniformity is taken into account parametrically:

$$\begin{aligned}S_0=&\frac{m_a}{t_2-t_1}(\mathbf{r}_2-\mathbf{r}_1)(\Delta\mathbf{r}_2-\Delta\mathbf{r}_1)-\frac{Z_ae}{\omega c(t_2-t_1)}\int_{\varphi_1}^{\varphi_2}\mathbf{A}\,\mathrm{d}\varphi\\&+\frac{Z_ae}{\omega c(t_2-t_1)}\frac{\mathbf{r}_2-\mathbf{r}_1}{t_2-t_1}\left(-\int_{\varphi_1-\Delta\varphi_1}^{\varphi_1+\Delta\varphi_1}\mathbf{A}\,\mathrm{d}\varphi+\int_{\varphi_2-\Delta\varphi_2}^{\varphi_2+\Delta\varphi_2}\mathbf{A}\,\mathrm{d}\varphi\right)\\&-\frac{Z_a^2e^2}{\omega^2m_a(t_2-t_1)}\\&\times\int_{\varphi_1}^{\varphi_2}\mathbf{A}\,\mathrm{d}\varphi\left(-\int_{\varphi_1-\Delta\varphi_1}^{\varphi_1+\Delta\varphi_1}\mathbf{A}\,\mathrm{d}\varphi+\int_{\varphi_2-\Delta\varphi_2}^{\varphi_2+\Delta\varphi_2}\mathbf{A}\,\mathrm{d}\varphi\right)\\&+\frac{Z_a^2e^2}{2\omega m_ac^2}\left(-\int_{\varphi_1-\Delta\varphi_1}^{\varphi_1+\Delta\varphi_1}\mathbf{A}^2\,\mathrm{d}\varphi+\int_{\varphi_2-\Delta\varphi_2}^{\varphi_2+\Delta\varphi_2}\mathbf{A}^2\,\mathrm{d}\varphi\right), \quad (23)\end{aligned}$$

where $\mathbf{A}=\mathbf{A}_0(\mathbf{r}_\perp,\varphi/\omega)\sin\varphi$ is the vector potential of the laser field, $\mathbf{r}_\perp\perp\mathbf{k}$, $\varphi_{1,2}=\omega t_{1,2}-\mathbf{k}\mathbf{r}_{1,2}$, $\Delta\varphi_{1,2}=-\mathbf{k}\Delta\mathbf{r}/2$, ω is the laser field frequency, and $\mathbf{k}$ is the wave vector.

In expression (22), ΔS_p is an addition to the action due to the ponderomotive forces that arise from the irregularity of the laser field amplitude A_0; the ponderomotive forces are included in accordance with the perturbation theory, which is applicable for sufficiently short times, during which the particle displacement is small in comparison with the characteristic irregularity dimension of the laser field amplitude A_0:

$$\Delta S_\mathrm{p}=-\frac{Z_a^2e^2}{4m_ac^2}\,\boldsymbol{\nabla}A_0^2\int_{t_1}^{t_2}\Delta\mathbf{r}_a\,\mathrm{d}t\,, \quad (24)$$

where $\Delta\mathbf{r}_a$ is the particle trajectory in a uniform field with the boundary conditions $\Delta\mathbf{r}_a(t_1)=\Delta\mathbf{r}_1$, $\Delta\mathbf{r}_a(t_2)=\Delta\mathbf{r}_2$.

The contribution ΔS_st to the action arising from particle interaction is given by (also calculated based on the perturbation theory)

$$\begin{aligned}\mathrm{Im}\,\Delta S_\mathrm{st}&=\pi\sum_b n_b\,\mathrm{V.p.}\int\mathrm{d}\mathbf{p}_b\,f_{1Z}(\mathbf{p}_b,t_1)\\&\times\int_{t_1}^{t_2}\mathrm{d}t\,\frac{Z_a(\mathbf{r}_1)e^2c^2}{\hbar}\,\frac{\bigl(\Delta\mathbf{r}_{a\perp\mathbf{v}_b}(t)\bigr)^2}{\mathbf{v}_b\Delta\dot{\mathbf{r}}_a(t)}\,,\\f_{1Z}(\mathbf{p}_b,t_1)&=\int\mathrm{d}\mathbf{r}\,f(\mathbf{r},\mathbf{p}_b,t_1)\,Z_b(\mathbf{r})\,,\end{aligned} \quad (25)$$

$$\begin{aligned}\mathrm{Re}\,\Delta S_\mathrm{st}&=-\pi\sum_b n_b\int\mathrm{d}\mathbf{p}_b\,f_{2Z}(\mathbf{p}_b,t_1)\\&\times\int_{t_1}^{t_2}\mathrm{d}t\,\frac{Z_a^2(\mathbf{r}_1)e^4}{\hbar v_b}\bigl(\Delta\mathbf{r}_{a\perp\mathbf{v}_b}(t)\bigr)^2,\\f_{2Z}(\mathbf{p}_b,t_1)&=\int\mathrm{d}\mathbf{r}\,f(\mathbf{r},\mathbf{p}_b,t_1)\,Z_b^2(\mathbf{r})\,,\end{aligned} \quad (26)$$

where Z_b, $\mathbf{p}_b$, $\mathbf{v}_b$, and n_b are the charge, momentum, velocity, and average density of the plasma particles of sort b. The calculations were carried out in accordance with expression (9) with the potential interaction energy

$$\begin{aligned}U_{ba}(\mathbf{r}_b-\mathbf{r}_a)&=Z_aZ_be^2\left(1-\frac{\dot{\mathbf{r}}_a\mathbf{v}_b}{c^2}\right)\\&\times\frac{1}{\sqrt{(\mathbf{r}_a-\mathbf{r}_b)^2(1-\dot{\mathbf{r}}_a^2/c^2)+\bigl[(\mathbf{r}_a-\mathbf{r}_b)\dot{\mathbf{r}}_a\bigr]^2/c^2}}\,,\end{aligned} \quad (27)$$

which accounts for both the scalar and vector field potentials of a plasma particle b (moving with a constant velocity) acting on a test particle of sort a. In deriving expressions (25) and (26), we also used the smallness of the laser field frequency in comparison with the characteristic (Weisskopf) variation frequency of the collision volume V_{ba}^st. The latter frequency is equal to the ratio between the characteristic velocity and the larger of the following two quantities: the Landau length and the de Broglie wavelength. We note that the imaginary part of the collision volume, which characterizes the broadening of the momentum distribution of particles a, is determined by the scalar potentials of perturbing particles.

When the initial distribution functions of plasma particles are given, their evolution may be found by multiple application of propagators (22)–(26). The statistically averaged in-plasma and scattered electromagnetic fields may be found from the plasma particle distribution functions [12]. The Fourier components of the energy densities of the longitudinal and transverse electric fields are given by

$$\begin{aligned}(\mathbf{E}_\parallel\mathbf{E}_\parallel)_{\omega,\mathbf{k}}&=\sum_a\frac{4\pi e^2n_a}{k^2}\,\frac{\int2\pi\delta(\omega-\mathbf{k}\mathbf{v})Z_a^2(\mathbf{R})f_a(\mathbf{R},\mathbf{p},t)\,\mathrm{d}\mathbf{p}}{\bigl|\varepsilon_\parallel(\omega,\mathbf{k})\bigr|^2}\,,\\(\mathbf{E}_\perp\mathbf{E}_\perp)_{\omega,\mathbf{k}}&=\sum_a\frac{4\pi e^2n_a}{k^2}\,\frac{\int2\pi\delta(\omega-\mathbf{k}\mathbf{v})(\mathbf{k}\times\mathbf{v})^2Z_a^2(\mathbf{R})f_a(\mathbf{R},\mathbf{p},t)\,\mathrm{d}\mathbf{p}}{\bigl|\omega^2\varepsilon_\perp(\omega,\mathbf{k})-c^2k^2\bigr|^2}\,,\\&\mathbf{E}_\parallel\parallel\mathbf{k},\quad\mathbf{E}_\perp\perp\mathbf{k}\,.\end{aligned} \quad (28)$$

The expressions for the longitudinal and transverse plasma permittivities are written as

$$\begin{aligned}\varepsilon_\parallel(\omega,\mathbf{k})&=1+\sum_a\frac{4\pi e^2n_a}{k^2\omega}\int\frac{(\mathbf{k}\mathbf{v})\mathbf{k}Z_a^2(\mathbf{R})\,\partial f_a(\mathbf{R},\mathbf{p},t)/\partial\mathbf{p}}{\omega-\mathbf{k}\mathbf{v}+\mathrm{i}0}\,\mathrm{d}\mathbf{p}\,,\\\varepsilon_\perp(\omega,\mathbf{k})&=1+\sum_a\frac{2\pi e^2n_a}{k^2\omega}\int\frac{\bigl((\mathbf{k}\times\mathbf{v})\times\mathbf{k}\bigr)Z_a^2(\mathbf{R})\,\partial f_a(\mathbf{R},\mathbf{p},t)/\partial\mathbf{p}}{\omega-\mathbf{k}\mathbf{v}+\mathrm{i}0}\,\mathrm{d}\mathbf{p}\,.\end{aligned} \quad (29)$$

In addition, we must calculate the average ion charges. For short femtosecond laser pulses, the ion charge at a given point is determined by the electric field strength of the laser field at this point [16] during the buildup of the laser field. When the laser field intensity decreases, the charge remains

invariable. This charge kinetics model is related to the overbarrier nature of ion ionization by a strong laser field and the short time of femtosecond laser pulse–target interaction. The laser field amplitude $E(t)$ and the ion charge Z are related by the Bethe formula [17] (in atomic units)

$$E(t) = \frac{I_{Z-1}^2}{4Z}\,, \tag{30}$$

where I_{Z-1} is the ionization potential of an ion with the charge $Z-1$. When the plasma field differs markedly from the laser field in a vacuum, the in-plasma electric-field energy density calculated in accordance with expression (28) must be used in (30). In the general case, when ionization is not of the overbarrier type, the average ion charges may be found from the charge kinetic equations that take both the ionization of atoms and ions by plasma electric fields and the electron collisions into account. Analytic expressions for the tunnel and overbarrier ionization rates and the ejected-electron momentum distributions were derived in Refs [18, 19] for nonrelativistic electrons and in Refs [20–22] for relativistic electrons. Expressions for the electron velocity distribution function for tunnel and multiphoton ionization by a relativistic laser field can be found in Ref. [23]. An analytic expression for the ionization rate in the multiphoton and overbarrier limit was derived in Ref. [24] for nonrelativistic electrons. We note that the investigation of ionization in plasmas may be complicated by the presence of quasistationary and alternating electric fields. The general analytic expression for the tunnel decay rate in the presence of a variable electric field (with the tunnel barrier produced by a constant electric field) was derived in Ref. [25].

The inclusion of ionization in the case of a high-intensity laser pulse leads to a small energy imbalance, which is corrected by adding the quantity

$$\frac{\mathrm{i}}{\hbar}\,\varepsilon(\mathbf{r}_2, t_2)(t_2 - t_1)$$

to the effective propagator action, where $\varepsilon(\mathbf{r}_2, t_2)$ is the energy required for ionizing atoms and ions.

4. Laser radiation absorption in plasma. Parametric instabilities

An electron embedded in a laser wave field executes an oscillatory motion. When the intensity is high enough ($I\lambda^2 \geqslant 10^{18}$ W cm^{-2} μm^{-2}), the oscillatory speed comes to be close to the speed of light. The laser radiation may be absorbed via energy transfer from the oscillatory motion to the translational motion of the electron. This transfer occurs as a result of inverse bremsstrahlung in the electron scattering by an atom [26–28], the stimulated and spontaneous Compton effect [28], and acceleration by the ponderomotive force in the motion in a nonuniform field [28–30]. The heating of plasma electrons due to the Compton effect prevails over the inverse bremsstrahlung in the dense plasma case, when the electron collision frequency is higher than the laser field frequency [28]. Electron heating in a nonuniform field is efficient when the nonuniformity is sufficiently strong, when the characteristic gradient scale length is shorter than the electron oscillation amplitude (ponderomotive scattering) [31–34]. In laser pulse–plasma interactions, the strong nonuniformity can result from either laser field scanning or the short rise time of the laser pulse.

Apart from the above mechanisms of laser field absorption by a plasma due to the scattering of laser pulse photons by electrons and the absorption of laser pulse photons by electrons in the presence of a 'third body' (ion, field irregularity), there is the anomalous absorption due to the parametric excitation of collective plasma motions (plasma waves). Parameters that characterize the plasma oscillate under the action of the laser field. This variation has the effect that, as in the case of mechanical vibratory systems, parametric resonance becomes possible, with the internal field of fluctuations increasing with time. The development of this parametric instability is inherent in the nature of the interaction between laser radiation and the plasma, which becomes turbulent.

The main elementary processes that determine the absorption of high-intensity laser radiation are the two-plasmon photon decay, stimulated Raman scattering, and stimulated Mandel'shtam–Brillouin scattering [3–6]. These processes are strongly affected by plasma nonuniformity, which is responsible for an increase in the threshold intensity of the parametric instability excitation and for the transfer of the energy of plasma waves to lower-density plasma regions [5]. Moreover, a sufficiently strong nonuniformity gives rise to a new absorption mechanism termed the plasma resonance [4, 35].

A two-plasmon decay involves the decay of a laser field photon into the quantum of a Langmuir plasma wave and an ion–sound wave quantum. The internal field emerging in the plasma is a potential field. This mechanism prevails in sufficiently dense plasmas for the electron densities $n > n_{\mathrm{cr}}/4$, $n_{\mathrm{cr}} = m_{\mathrm{e}}\omega^2/4\pi e^2$, where n_{cr} is the critical electron density. In a higher-density plasma, the electromagnetic wave with a frequency ω cannot propagate (for nonrelativistic intensities of the laser field).

When subpicosecond laser pulses propagate through a plasma, an important role is played by stimulated Raman scattering, whereby a laser field photon decays into the quantum of a Langmuir plasma wave and a transverse electromagnetic field quantum shifted in frequency. This instability is not potential. Stimulated Raman scattering is observed in a relatively tenuous plasma $n < n_{\mathrm{cr}}/4$ (see, e.g., Refs [4, 36]). At relativistic intensities, stimulated Raman scattering is also possible for higher densities due to the effective increase in the electron mass and the consequential decrease in the plasma frequency.

An ion–sound wave is excited in Mandel'shtam–Brillouin scattering. This process becomes significant for longer (nanosecond) pulses.

When relativistic effects (specifically, the oscillations of electron mass) are taken into account, two more parametric instabilities emerge: laser beam filamentation and laser beam modulation [6, 37]. As a result of the former instability, the laser beam splits into several laser beams with a higher intensity (transverse nonuniformity), and the modulation instability has the effect that the laser beam intensity becomes nonuniform in the direction of its propagation. The emergence of the relativistic filamentation of a laser beam is explained as follows. The dispersion relation for the transverse electromagnetic wave in a plasma, with the relativistic oscillation of the electron mass taken into account, results in the phase velocity of the wave being lower at the point where the intensity is higher. This leads to a wavefront flexure and the consequential increase in the focusing intensity of the laser beam in the direction of its

propagation. The occurrence of the relativistic modulation instability may be described as follows. The superposition of the electron plasma wave and the laser pump wave results in an electric field in the form of a shifted sinusoidal wave. Due to the relativistic mass oscillation, the electrons become lighter near the minimum of the field and heavier near the peak. As a result, the faster plasma oscillations near the minimum are dephased relative to the oscillations near the maximum of the field. This increases the density modulation and leads to relativistic instability [6]. It is worth noting that the ponderomotive force has a marked effect on the character of the modulation instability in a weakly relativistic plasma [6]. Also worthy of mention is the anisotropy of the filamentation instability of a linearly polarized laser beam at near-critical plasma densities [38, 39].

In high-intensity laser fields, in which the electron motion is relativistic, these instabilities merge with stimulated Raman scattering and two-plasmon decay [40]. The presence of high-energy electrons accelerated by the plasma wave exerts an appreciable effect on the parametric instabilities: the instability increment decreases, the instability domain in the wave-vector space is shifted, and the frequency spectrum of the Raman scattering changes [41].

The inclusion of relativistic effects and of ion motion is important for simulations of the resonance absorption of the laser field [42, 43]. In the nonuniform plasma case (with the density gradient scale length of the order of several wavelengths), a resonance is observed in the angular dependence of absorption of a p-polarized laser pulse obliquely incident on the plasma.

The absorption of high-intensity laser radiation at a sharp vacuum – plasma boundary may occur due to the 'vacuum heating' [44] and $\mathbf{j} \times \mathbf{B}$ heating [45, 46] of electrons. The 'vacuum heating' of electrons occurs when a p-polarized laser pulse is obliquely incident on the vacuum – plasma interface. The electric field of the laser pulse ejects electrons from the plasma surface to force them into the plasma half a period later. However, they are heated due to either the strongly inelastic inverse bremsstrahlung or the ponderomotive scattering. In the $\mathbf{j} \times \mathbf{B}$ heating case, the electrons that oscillate near the plasma surface in the electric field of a laser pulse incident normally on the vacuum – plasma interface are forced into the plasma by the magnetic field of this laser pulse. This occurs every half period of the laser pulse. The $\mathbf{j} \times \mathbf{B}$ heating results in the production of a modulated electron beam, whose transition radiation is observed at the rear target surface. The transition radiation at the double frequency of the laser pulse has been experimentally observed [47], which confirms the $\mathbf{j} \times \mathbf{B}$-heating mechanism of electron acceleration in the plasma. The 'vacuum heating' of electrons in the plasma at oblique incidence of a laser pulse was indirectly borne out in the experiment in Ref. [48] in the measurement of the absorption coefficient.

5. Relativistic subpicosecond laser pulse – plasma interaction

5.1 Wake wave

When a laser pulse passes through a tenuous ($n \ll n_{cr}$) plasma, a wake wave is excited behind the pulse front [49 – 52], which entrains and accelerates the plasma electrons. This principle underlies the operation of the laser particle accelerator (see review Refs [53 – 55]), whose main advantage is its compactness. The wake wave is excited only when the leading edge of the laser pulse is steep [52]. Its physical excitation mechanism is reliant on the ponderomotive force of the laser pulse, which results in an electron density perturbation. The charge separation field drives a charge density wave behind the laser pulse. A characteristic feature of the wake wave consists in the potential of its electric field (for relativistic intensities of the laser pulse and a sufficiently steep leading edge) being far greater that the potential of the laser wave field, the potential of the wake wave increasing with the plasma density. But the longitudinal electric intensity of the wake wave cannot exceed a certain maximum value, which depends on the plasma parameters and the velocity of electron oscillations in the laser field (a one-dimensional theory was elaborated in Ref. [56]). The wake wave breaks down for higher intensities of the longitudinal electric field.

Relativistic laser pulses are characterized by a strong ponderomotive force, which produces a laser channel with a lowered electron density in the plasma. The number of periods in the wake wave behind the laser pulse edge may be determined by its breaking due to the transverse nonuniformity of the plasma frequency in the laser channel [57]. The nonuniformity leads to an increase in the curvature of the wake wave front with the distance from the laser pulse. When the electron oscillation amplitude becomes equal to the curvature radius, the wave front becomes ambiguous (wave breaking) and the plasma electric field is no longer regular. The electron trajectories then become self-intersecting. In the severe breaking of the wake wave, the process of stimulated Raman scattering prevails.

Another reason for the front curvature increase in the wake wave responsible for its breaking is the formation of a small-scale structure in the laser channel, which is due to the action of the ponderomotive force of the wake wave itself [58].

The wake wave is most efficiently excited by a laser pulse with the wavelength equal to half the wavelength of the plasma wave [53, 54]. When longer laser pulses propagate through the plasma, efficient generation of the wake wave is possible as a result of the development of a laser-pulse self-modulation instability caused by stimulated Raman scattering in the direction of the laser wave. The self-modulation may stem from two effects. First, the electron density fluctuations related to the plasma wave lead to changes in the group velocity, leading to a longitudinal modulation of the laser pulse. The laser pulse splits into a sequence of short pulses with lengths equal to half the wavelength of the plasma wave. Second, the density fluctuations act as positive and negative lenses to give rise to laser beam self-focusing. The self-focusing and the self-modulation may emerge concurrently. In the passage of a laser pulse through a gas (but not through a preformed plasma), self-modulation also emerges due to excitation of a seed wake wave [59]. This wave is generated due to a sharpening of the leading laser-pulse edge by ionization modulation.

Both the electron density modulation and the acceleration of plasma electrons by the wake wave have been experimentally observed [53 – 55]. The highest electron energy obtained in experiments is equal to 200 MeV.

5.2 Stimulated Raman scattering

In the case of the plasma density high enough for the wake wave to break up, the main process determining the nature of the interaction between relativistic subpicosecond laser pulses and the plasma is the stimulated Raman scattering. Back-

scattering and forward scattering, whereby the laser wave (of frequency ω) decays into a plasma electron wave (of frequency ω_p) and an electromagnetic wave (with the Stokes frequency $\omega - \omega_p$), which propagates in the direction of the laser wave, are recognized. In the backscattering, the electromagnetic wave propagates in the opposite direction relative to the laser wave. Merging of the laser and plasma waves, resulting in the generation of waves with the anti-Stokes frequency $\omega + \omega_p$, also occurs. In the scattering of a relativistic laser pulse, a broad spectrum of Stokes ($\omega - N\omega_p$) (N is an integer) and anti-Stokes ($\omega + N\omega_p$) frequencies emerges, which was observed in experiments [60, 61].

The plasma waves produced due to stimulated Raman scattering accelerate the plasma electrons. Unlike with the acceleration driven by the wake wave, the spectrum of electrons accelerated due to Raman scattering is broad and Maxwellian in nature. With an increase in the relativistic intensity of laser pulses, saturation of the increment of stimulated Raman scattering [62] and hence of the yield of accelerated electrons [61] occurs.

In the backscattering of relativistic laser pulses, a high-intensity electromagnetic wave propagating in the opposite direction arises. Under these conditions, the electron dynamics may become stochastic and electrons may be stochastically accelerated [63] if the scattered wave is strong enough. The stochastic heating of plasma electrons in the field of counterpropagating waves was observed in numerical simulations [64, 65].

The passage of relativistic laser pulses through the plasma is characterized by the production of lower-density channels. They are produced by the ponderomotive force caused by nonuniformity of the laser beam intensity. The production of lower-density channels in the stimulated Raman scattering of laser pulses was observed in the experiments in Refs [66, 67], as well as in experimental and computational work [68]. The transmission factor increases with the intensity of laser pulses [66, 69]. The enhancement of transmittance is attributable to weakening of stimulated Raman scattering in the channel due to the generation of hot electrons (with temperatures ranging into the megaelectronvolts) [69, 70]. High-energy ions (helium nuclei) traveling in the radial direction were discovered in Ref. [67]. Their acceleration was caused by the Coulomb repulsive force (Coulomb explosion) in the electron-depleted channel. The total fast-ion energy accounts for 6% of the laser pulse energy.

5.3 Laser-beam filamentation

On further increase in plasma density, the single laser channel splits into several channels owing to the relativistic self-focusing instability. This is clearly shown by the numerical simulations of laser pulse transit through a plasma [71 – 74]. The self-focusing of the laser beam is also fostered by the ponderomotive ejection of electrons from the beam axis, with the medium acting as a positive lens in this case. Owing to parametric instabilities, electron plasma waves are excited in the plasma, which accelerate electrons to produce streams of hot electrons. The Weible instability [75] tends to break these electron currents, resulting in the formation of filaments of fast electrons and reverse currents caused by slow electrons [76]. The fast-electron currents generate a strong magnetic field, whose maximum amplitude is comparable to the magnetic field of the laser wave. It was discovered in Ref. [76] that this magnetic field pinches the current of fast electrons. The laser beam is deflected following the fast electrons with the formation of a common channel for the propagation of the laser pulse and the current of the fast electrons. The laser beam intensity increases by about an order of magnitude. The magnetic mechanism of channel merging was confirmed by simulations involving an applied external magnetic field. In the three-dimensional case, this effect was investigated in Ref. [71]. Also noted in this paper was a lowering of the ion density on the beam axis and an ion acceleration in the radial direction (up to the energy 3 MeV for the intensity 10^{19} W cm^{-2}) caused by the ponderomotive ejection of electrons from the laser beam axis.

Observed in the filamentation of a laser beam is an increase in both the length of the laser channel in the plasma and the high-energy electron heating. An experimental observation of an increase in the hot-electron temperature with increasing the plasma density was reported in Ref. [77]. This increase is attributable to the progressively higher ratio between the laser pulse power and the threshold power for the relativistic self-focusing instability. The calculation carried out in Ref. [77] suggests that electron heating is effected by the transverse electromagnetic field of the laser pulse. The mechanism of this heating was proposed in Ref. [78]: it was shown that in the presence of a weak random force acting in the transverse direction, electron acceleration in the longitudinal direction of laser wave propagation occurs. A weak random force leads to dephasing of electron oscillations in the laser wave and to electron heating by a mechanism similar to the inverse bremsstrahlung. The dephasing may occur in transverse motion of electrons that fall out of laser filaments.

5.4 Passage of laser pulses through a supercritical plasma

When a relativistic laser pulse is normally incident on the plasma with a density much higher than the critical one, the light pressure force results in the formation of a lower-density plasma channel, which is transparent for the laser pulse (see the data of simulations [79] and experiment [80]).

When a relativistic laser pulse is normally incident on a nonuniform plasma, a resonance in its absorption occurs [81]. The absorption coefficient has a local peak when the density gradient is optimum for a given laser intensity. The resonance is attributable to distortion of the electron plasma density and the subsequent enhancement of the ponderomotive absorption.

When a channel is formed in a supercritical-density plasma, the laser pulse departs from the initial direction of propagation (see the numerical simulations in Ref. [82]). The beam of hot electrons accelerated in the plasma is accordingly deflected. When a laser pulse was incident on a solid gold target, the beam of hot relativistic electrons (with the average energy several times higher than the ponderomotive energy of electrons in the laser field) was observed to fluctuate in direction in the experiments reported in Ref. [83].

In the passage of a laser pulse through a supercritical plasma, a substantial part (40 – 50%) of the laser pulse energy transforms into the energy of hot electrons. This is evident both from 'particle-in-cell' simulations [71, 76, 79] and from experimental data [83]. High-intensity beams of hot electrons are proposed for use in the fast ignition of thermonuclear targets [84], as well as a source of γ-ray photons generated due to electron bremsstrahlung [85]. These γ-ray photons of an electromagnetic field may be used in radiography [82], for the initiation of photonuclear reactions [86], and for the production of electron – positron pairs [86 – 91].

We consider the interaction between a supercritical plasma and a linearly polarized laser pulse with the envelope

$$A_{0x} = A_0 \exp\left(-\frac{(t - z/c)^2}{\tau^2}\right) \exp\left(-\frac{x^2 + y^2}{\sigma^2}\right), \qquad (31)$$

with the z axis aligned with the wave vector of the laser pulse and the x axis aligned with the polarization axis. The electron density distribution is given by

$$n_e(z) = n_{cr} \exp\frac{z}{L}, \quad 0 < z < z_{max}, \qquad (32)$$

where $n_{cr} = \pi m_e c^2/e^2\lambda^2$ is the critical density: when the critical density is exceeded, the wave can no longer propagate through the plasma (for nonrelativistic intensities). The above density distribution sets in due to the ablation of a solid target under prepulse irradiation. In addition, the plasma heats up to a temperature about 1 keV.

In the pursuance of calculations, we can conveniently pass to the purely coordinate representation in formulas (25) and (26) in accordance with (21). All integrals in formulas (25) and (26) were calculated by the stationary phase method (in the multidimensional case) [92]. They belong to the type of integrals of rapidly oscillating functions because the plasma is classical (nondegenerate) in the case under discussion.

Initial simulations were carried out for a hydrogen plasma with the same pulse parameters and degree of plasma nonuniformity as in Ref. [93]: $\tau = 150$ fs, $\sigma = 6\lambda$, $L = 30\lambda$ ($\lambda = 1$ μm is the wavelength of the laser pulse). The computation range was somewhat shorter: $z_{max} = 40\lambda$. The simulations were performed for peak intensities $I_0 = 10^{18}$, 10^{19}, and 10^{20} W cm^{-2}. The electron momentum z-component distribution for $I_0 = 10^{20}$ W cm^{-2} is depicted in Fig. 1. It is mainly in this direction that electrons experience acceleration. The results of calculations are consistent with the data in Ref. [93]. Indeed, for the intensity $I_0 = 10^{18}$ W cm^{-2}, fast electrons are heated to the temperature $T_h \sim 0.8$ MeV, for $I_0 = 10^{19}$ W cm^{-2} to $T_h \approx 4.5$ MeV in the energy range below 12.5 MeV (the average $T_h \approx 8$ MeV in the energy range below 50 MeV), for $I_0 = 10^{20}$ W cm^{-2} to $T_h \approx 15$ MeV in the energy range above 25 MeV, and the respective fast-electron temperatures in Ref. [93] lie in the ranges 0.5 – 1.2 MeV, 3 – 8 MeV, and 9 – 16 MeV. Figure 1 clearly shows the occurrence of fast electrons traveling in the opposite direction. This

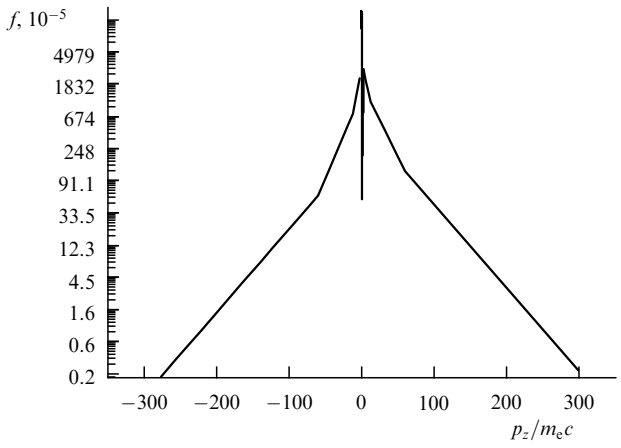

Figure 1. Electron momentum z-component distribution function for $I_0 = 10^{20}$ W cm^{-2}.

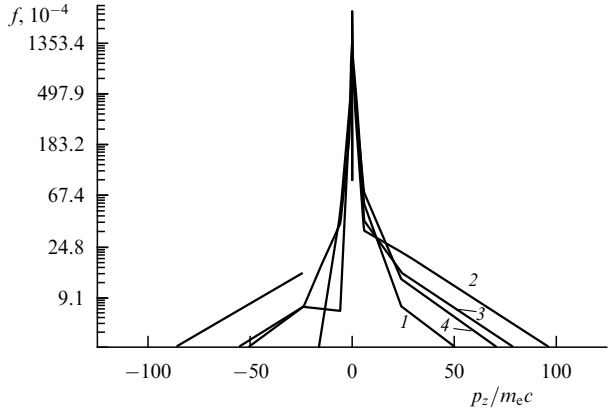

Figure 2. Electron momentum z-component distribution function for $I_0 = 10^{19}$ W cm^{-2} taken at consecutive instants: *1* — $t = 45\,T$, *2* — $t = 46\,T$, *3* — $t = 47\,T$, *4* — $t = 48\,T$ (T is the laser field period, the initial time instant is $t_0 = -50\,T$).

occurs due to the development of a Weible instability of the anisotropic electron momentum distribution in the plasma [75]. In addition, thermal electrons are heated to temperatures of the order of 10 keV due to anomalous conductivity.

To gain an insight into the electron acceleration mechanism, we consider the variation of the momentum z-component distribution function at earlier instants, prior to the settling of the stationary distribution. Figure 2 shows this distribution function at consecutive instants (for $I_0 = 10^{19}$ W cm^{-2}). We can see irregular variations with time caused by turbulent pulsations of the plasma field. Therefore, electrons are primarily accelerated by the turbulent pulsations of the plasma field by a mechanism similar to Fermi acceleration [94]. The acceleration mechanism discovered in Ref. [93], related to the mechanical resonance between electron betatron oscillations in quasistationary magnetic and electric fields and the laser field, is not the dominant one.

Figure 1 shows clearly that the momentum distribution of hot electrons has a two-temperature form. This may be attributed to the combined action of both the ponderomotive force and the turbulent plasma field, specifically, to ponderomotive-force acceleration of the tail of electrons already accelerated by the plasma field.

Simulations were also carried out for a plasma of multiply charged gold ions for peak intensities $I_0 = 10^{20}$ W cm^{-2} and $I_0 = 3 \times 10^{20}$ W cm^{-2}. At these intensities, gold atoms ionize to the charge $Z_i = 51$ according to Bethe formula (30). This charge is close to the equilibrium charge at characteristic temperatures about 300 – 500 eV and the critical density. The following parameters were taken in formulas (31) and (32): $\tau = 150$ fs, $\sigma = 9\lambda$, $L = 20\lambda$ ($\lambda = 1$ μm), and $z_{max} = 60\lambda$. The calculated data are shown in Fig. 3. In the 10 – 25 MeV energy range, electrons are heated to the temperature $T_h \approx 10$ MeV, which is consistent with the estimate $T_h \sim 4 \pm 1$ MeV obtained experimentally in Ref. [83]. The results of the last-mentioned calculations are also in agreement with some of the experimental data in Ref. [86], the discrepancy between the parameters of the distribution functions being less than 25%. Indeed, the energy distribution of hot electrons measured at an angle of 30° has a two-temperature form: $T_h \cong 7$ MeV in the range from 10 to 30 MeV and $T_h \cong 20$ MeV in the range from 40 to 100 MeV; in Fig. 3, $T_h \cong 8.6$ MeV (making allowance for the observation angle of 30°) in the 10 –

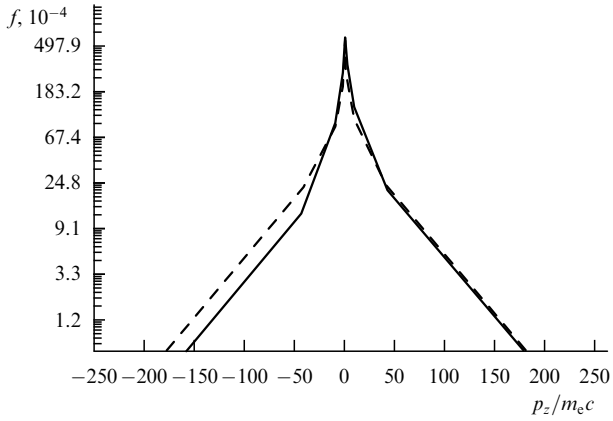

Figure 3. The electron momentum z-component distribution function for $I_0 = 10^{20}$ W cm^{-2} (solid line) and $I_0 = 3 \times 10^{20}$ W cm^{-2} dashed line) in a plasma with multiply charged gold ions.

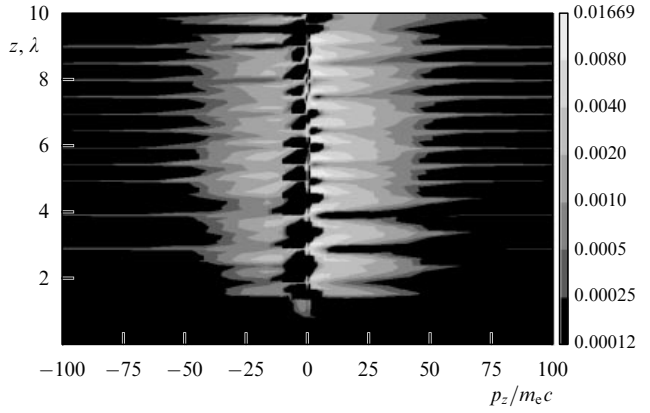

Figure 4. Electron distribution in the (y, p_z) phase plane.

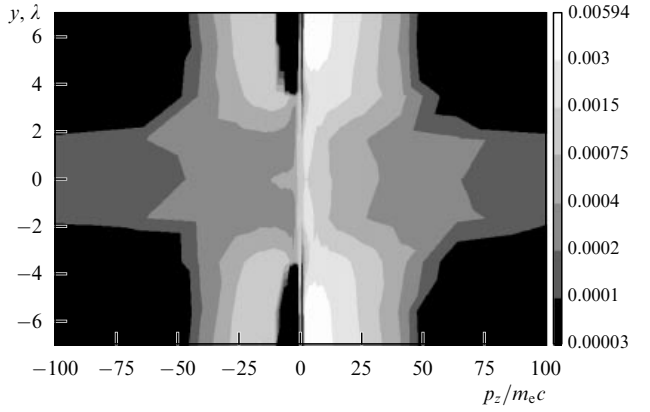

Figure 5. Electron distribution in the (z, p_z) phase plane.

25 MeV range and $T_h \cong 20$ MeV in the 25 – 90 MeV range. As in the case of a hydrogen plasma, electrons are accelerated by turbulent pulsations of the plasma field. Thermal electrons are heated to a temperature about 10 keV due to anomalous plasma conductivity. All these calculations were made with a Pentium-4 class PC.

5.5 A nonuniform plasma with sharp boundaries

A nonuniform plasma with sharp boundaries emerges either in the interaction of relativistic laser pulses with a thin solid target or when a pulse with a high contrast ratio (with a weak prepulse) is incident on a thick target. This interaction results in the production of high-intensity fast ion beams (primarily protons), which have been observed in numerous experiments [83, 86, 95 – 114] and in particle-in-cell simulations [114 – 128]. Energy-wise investigations are made of the angular distribution of fast ions, which may be used for the fast ignition of a thermonuclear target [129 – 131], protonographic diagnostics of fast processes in plasmas [132, 133], isochoric heating of a solid with the aim of obtaining high pressures [134] or a neutron source [96, 114, 135, 136], initiating nuclear reactions [137], and investigating neutrino oscillations [138].

The scenario of proton acceleration in the interaction of a high-intensity femtosecond laser pulse with a thin target is as follows. The ponderomotive force accelerates electrons, with the consequence that charge separation occurs near both the front and rear target boundaries. The resultant ambipolar electric field accelerates the ions in the plasma of the target. Additional acceleration may arise from the Coulomb ion explosion [115] and the vortex electric field [116]. An efficient stochastic mechanism of electron acceleration also exists [64, 65], whereby optimum conditions for proton acceleration emerge [126]. The collisionless electrostatic shock wave produced by the strong ponderomotive force may also be responsible for efficient ion acceleration [46, 128]. Ions may be accelerated both near the front side of a thin target [96, 97, 105, 118, 119] and near its rear side [83, 99, 104, 112, 115, 116, 120]. In the simulations reported in Ref. [127], the accelerating ambipolar field is distributed over a broad region. When a laser pulse is incident on a thick target, ions are also accelerated due to the ambipolar field [102, 124] arising from the action exerted on electrons by the ponderomotive force of both the incident and reflected laser pulses. It is pertinent to note that the accelerated-ion energy distribution depends on the ejected-electron distribution function. For a free plasma expansion in a vacuum, this was demonstrated in Refs [114, 139, 140].

In what follows, we consider the interaction between a linearly polarized laser pulse with envelope (31) and aluminum foil [141]. The laser pulse parameters are $\tau = 20T$, $\sigma = 7\lambda$, and $\lambda = 0.8$ μm, where T and λ are the period and wavelength of the laser pulse. The peak intensity is as high as $I_0 = 10^{20}$ W cm^{-2}. The angle the laser wave vector makes with the normal to the plane of the foil is equal to 22°, as in the experiment in Ref. [104]. The foil thickness is 3 μm and the initial electron and Al^{13+} ion densities correspond to the solid-state density. There are also hydrogen impurity ions.

Given the initial distribution functions of plasma particles, their evolution may be found by means of multiple, sequential application of propagators (22) – (26) in accordance with relation (10). To investigate the generation of fast protons, three sorts of particles are to be considered: electrons, target ions, and hydrogen impurity ions.

On the whole, the interaction proceeds as in particle-in-cell simulations. The strong ponderomotive force of the laser pulse ejects and accelerates electrons along its direction of propagation, resulting in a strong charge separation. The electron distributions in the phase planes (z, p_z) and (y, p_z) are depicted in Figs 4 and 5, respectively. These distributions are given for the instant of cessation of laser pulse – target

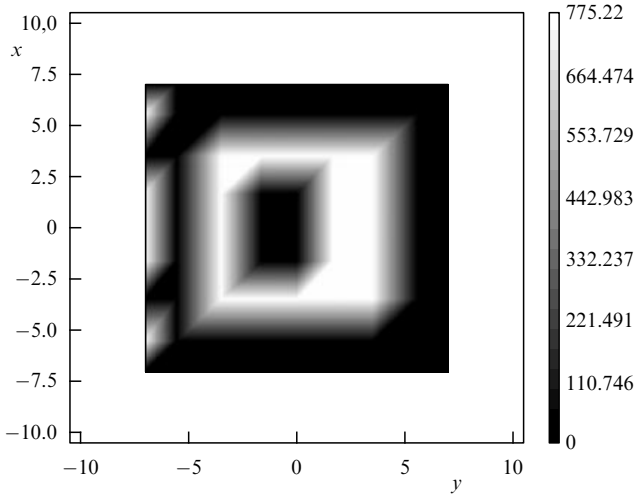

Figure 6. Three-dimensional representation of the electron density in units of 10^{21} cm^{-3}.

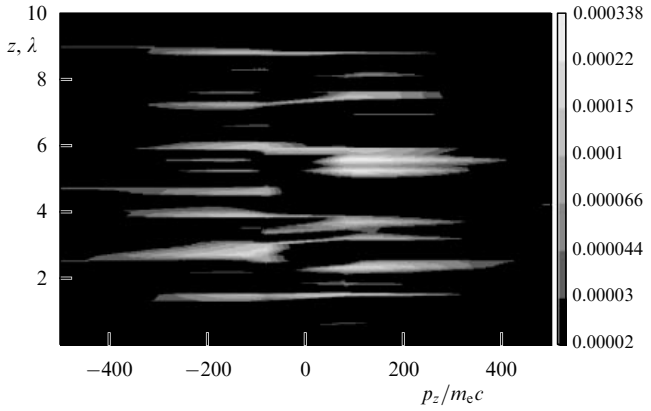

Figure 7. Fast-proton distribution in the (z, p_z) phase plane.

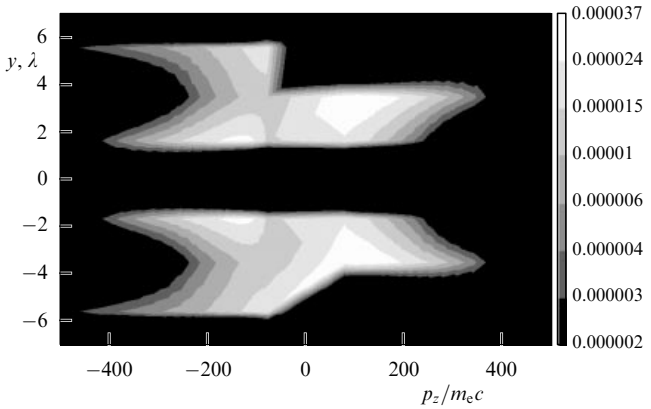

Figure 8. Fast-proton distribution in the (y, p_z) phase plane.

interaction. It can be seen from Figs 4 and 5 that the electrons are accelerated to relativistic velocities in the direction of pulse propagation. The development of a Weible instability [75] is responsible for the generation of an oppositely directed electron current. The averaged description (the characteristic scale length is of the order of the wavelength) of this instability is given in Fig. 5. Normally, the Weible instability develops to smaller scales [142].

The electron density distribution at the instant of cessation of the laser pulse – target interaction is shown in Fig. 6. It can be seen that electron detachment at the target center occurs, the electron density in the detached parts remaining close to the solid-state density. In particle-in-cell simulations, relativistic electrons make up a tenuous halo around the target (see, e.g., Refs [104, 119, 120], but the initial electron density assumed in these papers is an order of magnitude lower than the solid-state density).

The ambipolar electric field produced due to charge separation accelerates ions and impurity protons, primarily the impurity protons being accelerated. If the initial proton and aluminum ion densities are equal, the fast-proton temperature $T_{\rm ph} = 4$ MeV and the total number of accelerated protons with energies above 1 MeV is approximately equal to 3.5×10^{11} (the uncertainty of calculation is $\sim 20\%$). These data are consistent with the experimental data in Ref. [104], which reported the temperature $T_{\rm ph} = 3.2 \pm 0.3$ MeV and the number of accelerated protons 1.6×10^{11}. The total number of accelerated protons depends heavily on their initial relative density in the target: for a proton fraction of 3%, the number of accelerated protons decreases to 0.5×10^{10}. The discrepancy in the number of accelerated protons stems from the fact that the initial proton density in the target is unknown.

From the fast-proton distribution in the (z, p_z) phase plane shown in Fig. 7, it is evident that the majority of protons are accelerated in the region $z = (5-6)\lambda$, which is close to the value of z at which the plane $x = 0$ intersects the rear target boundary. Consequently, protons are accelerated primarily near the rear side of the target, which corresponds to the data of simulations in Ref. [104].

An interesting feature of the in-target proton acceleration is its absence near $y = 0$ (Fig. 8). This is supposedly due to the intense reverse current of relativistic electrons near this value of y (see Fig. 5). The simulations were carried out on a Pentium-4 class PC.

6. Conclusion

A kinetic theory of tenuous plasmas and gases has been developed, which involves construction of a distribution function propagator dependent on this distribution function. An analytic expression has been obtained for the propagator describing the evolution of a classical Coulomb plasma in the field of a high-intensity short laser pulse for times shorter than the relaxation time. This theory was used to investigate the generation of fast electrons by relativistic femtosecond pulses in plasmas with densities of the order of and higher than the critical density, as well as the interaction of a relativistic ($I_0 = 10^{20}$ W cm^{-2}) femtosecond laser pulse with thin aluminum foil. The new computational technique enables carrying out simulations for realistic large ion charges and high plasma densities. In some cases, three-dimensional calculations become feasible with a personal computer.

High-energy electron and ion streams obtained under different regimes of the relativistic laser pulse–plasma interaction may be used for the fast ignition of a thermonuclear target, the production of high pressures, X-ray and protonographic diagnostics of fast processes in plasmas and neutron sources, the initiation of nuclear reactions, and electron–positron pair production. Furthermore, the pre-

sently existing terawatt lasers offer promise as compact accelerators of electrons and ions.

Applying the new method to some problems of relativistic laser pulse–plasma interaction has led to a reinterpretation of the calculations in the case of hot-electron generation in supercritical-density plasmas and to a somewhat different regime of interaction with a thin target. The momentum distributions of hot electrons and fast protons obtained in this case are consistent with simulations by the standard particle-in-cell method and with experimental data. By and large, the numerical simulations of laser-produced plasmas carried out by the particle-in-cell method are in qualitative agreement with experimental data. These simulations are, as a rule, performed involving model plasmas with lower ion charges and densities. The method elaborated here holds promise for investigations of the kinetics of laser-produced plasmas with multiply charged ions and the kinetics of the interaction between laser pulses and dense plasmas. Plasmas of this kind emerge in the interaction of high-intensity laser pulses with heavy gases and solid targets.

References

1. Mourou G A, Barty C P J, Perry M D *Phys. Today* **51** (1) 22 (1998)
2. Kryukov P G *Kvantovaya Elektron.* **31** 95 (2001) [*Quantum Electron.* **31** 95 (2001)]
3. Silin V P *Parametricheskoe Vozdeistvie Izlucheniya Bol'shoi Moshchnosti na Plazmu* (Parametric Action of High-Power Radiation on Plasma) (Moscow: Nauka, 1973)
4. Kruer W L *The Physics of Laser Plasma Interactions* (Frontiers in Physics, Vol. 73) (Redwood City, Calif.: Addison-Wesley, 1988)
5. Silin V P, Tikhonchuk V T *Phys. Rep.* **135** 1 (1986)
6. Shukla P K et al. *Phys. Rep.* **138** 1 (1986)
7. Pukhov A *Rep. Prog. Phys.* **66** 47 (2003)
8. Sigov Yu S *Vychislitel'nyi Eksperiment: Most mezhdu Proshlym i Budushchim Fiziki Plazmy. Izbrannye Trudy* (Computing Experiment: a Bridge between the Past and Future of Plasma Physics. Selected Works) (Comp. G I Zmievskaya, V D Levchenko) (Moscow: Fizmatlit, 2001)
9. Lifshitz E M, Pitaevskii L P *Fizicheskaya Kinetika* (Physical Kinetics) (Moscow: Nauka, 1979) [Translated into English (Oxford: Pergamon Press, 1981)]
10. Kosarev I N *Zh. Tekh. Fiz.* **74** (4) 133 (2004) [*Tech. Phys.* **49** 509 (2004)]
11. Kosarev I N *Zh. Tekh. Fiz.* **75** (1) 32 (2005) [*Tech. Phys.* **50** 30 (2005)]
12. Klimontovich Yu L *Kineticheskaya Teoriya Neideal'nogo Gaza i Neideal'noi Plazmy* (Kinetic Theory of Nonideal Gases and Nonideal Plasmas) (Moscow: Nauka, 1975) [Translated into English (Oxford: Pergamon Press, 1982)]
13. Feynman R P, Hibbs A R *Quantum Mechanics and Path Integrals* (New York: McGraw-Hill, 1965) [Translated into Russian (Moscow: Mir, 1968)]
14. Griem H R *Plasma Spectroscopy* (New York: McGraw-Hill, 1964) [Translated into Russian (Moscow: Atomizdat, 1969)]; Sobel'man I I *Vvedenie v Teoriyu Atomnykh Spektrov* (Introduction to the Theory of Atomic Spectra) (Moscow: Fizmatgiz, 1963) [Translated into English (Oxford: Pergamon Press, 1972)]
15. Landau L D, Lifshitz E M *Teoriya Polya* (The Classical Theory of Fields) (Moscow: Nauka, 1973) [Translated into English (Oxford: Pergamon Press, 1975)]
16. Krainov V P, Roshchupkin A S *Phys. Rev. A* **64** 063204 (2001)
17. Bethe H A, Salpeter E E *Quantum Mechanics of One- and Two-electron Atoms* 2nd ed. (New York: Plenum/Rosetta, 1977)
18. Delone N B, Krainov V P *J. Opt. Soc. Am. B* **8** 1207 (1991)
19. Krainov V P *J. Opt. Soc. Am. B* **14** 425 (1997)
20. Krainov V P *J. Phys. B: At. Mol. Opt. Phys.* **32** 1607 (1999)
21. Krainov V P *J. Phys. B: At. Mol. Opt. Phys.* **36** L169 (2003)
22. Milosevic N, Krainov V P, Brabec T *Phys. Rev. Lett.* **89** 193001 (2002)
23. Hafizi B et al. *Phys. Rev. E* **67** 056407 (2003)
24. Kosarev I N *Opt. Spektrosk.* **101** 357 (2006) [*Opt. Spectrosc.* **101** 335 (2006)]
25. Kosarev I N, Yudin G L *Phys. Lett. A* **160** 443 (1991)
26. Silin V P *Zh. Eksp. Teor. Fiz.* **47** 2254 (1964) [*Sov. Phys. JETP* **20** 1510 (1965)]
27. Silin V P *Zh. Eksp. Teor. Fiz.* **111** 478 (1997) [*JETP* **84** 262 (1997)]
28. Fedorov M V *Elektron v Sil'nom Svetovom Pole* (Electron in a Strong Light Field) (Moscow: Nauka, 1991)
29. Bituk D R, Fedorov M V *Zh. Eksp. Teor. Fiz.* **116** 1198 (1999) [*JETP* **89** 640 (1999)]
30. Salamin Y I, Keitel C H *Phys. Rev. Lett.* **88** 095005 (2002)
31. Hartemann F V et al. *Phys. Rev. E* **51** 4833 (1995)
32. Malka G, Lefebvre E, Miquel J L *Phys. Rev. Lett.* **78** 3314 (1997)
33. Narozhny N B, Fofanov M S *Zh. Eksp. Teor. Fiz.* **117** 867 (2000) [*JETP* **90** 753 (2000)]
34. Narozhny N B, Fofanov M S *Phys. Lett. A* **295** 87 (2002)
35. Ginzburg V L *Rasprostranenie Elektromagnitnykh Voln v Plazme* (The Propagation of Electromagnetic Waves in Plasmas) (Moscow: Fizmatgiz, 1960) [Translated into English (Oxford: Pergamon Press, 1964)]
36. Estabrook K, Kruer W L *Phys. Fluids* **26** 1892 (1983)
37. Max C E, Arons J, Langdon A B *Phys. Rev. Lett.* **33** 209 (1974)
38. Honda T et al. *J. Plasma Fusion Res.* **75** 219 (1999)
39. Sheng Z-M et al. *Phys. Rev. E* **64** 066409 (2001)
40. Quesnel B et al. *Phys. Rev. Lett.* **78** 2132 (1997)
41. Sheng Z-M et al. *Phys. Rev. E* **61** 4362 (2000)
42. Estabrook K G, Valeo E J, Kruer W L *Phys. Fluids* **18** 1151 (1975)
43. Estabrook K, Kruer W L *Phys. Rev. Lett.* **40** 42 (1978)
44. Brunel F *Phys. Rev. Lett.* **59** 52 (1987)
45. Kruer W L, Estabrook K *Phys. Fluids* **28** 430 (1985)
46. Denavit J *Phys. Rev. Lett.* **69** 3052 (1992)
47. Baton S D et al. *Phys. Rev. Lett.* **91** 105001 (2003)
48. Grimes M K et al. *Phys. Rev. Lett.* **82** 4010 (1999)
49. Tajima T, Dawson J M *Phys. Rev. Lett.* **43** 267 (1979)
50. Gorbunov L M, Kirsanov V I *Zh. Eksp. Teor. Fiz.* **93** 509 (1987) [*Sov. Phys. JETP* **66** 290 (1987)]
51. Sprangle P et al. *Appl. Phys. Lett.* **53** 2146 (1988)
52. Bulanov S V, Kirsanov V I, Sakharov A S *Pis'ma Zh. Eksp. Teor. Fiz.* **50** 176 (1989) [*JETP Lett.* **50** 198 (1989)]
53. Esarey E et al. *IEEE Trans. Plasma Sci.* **24** 252 (1996)
54. Andreev N E, Gorbunov L M *Usp. Fiz. Nauk* **169** 53 (1999) [*Phys. Usp.* **42** 49 (1999)]
55. Bingham R, Mendonça J T, Shukla P K *Plasma Phys. Control. Fusion* **46** R1 (2004)
56. Katsouleas T, Mori W B *Phys. Rev. Lett.* **61** 90 (1988)
57. Bulanov S V et al. *Phys. Rev. Lett.* **78** 4205 (1997)
58. Gorbunov L M, Mora P, Solodov A A *Phys. Plasmas* **10** 1124 (2003)
59. Andreev N E, Chegotov M V, Pogosova A A *Zh. Eksp. Teor. Fiz.* **123** 1006 (2003) [*JETP* **96** 885 (2003)]
60. Darrow C B et al. *Phys. Rev. Lett.* **69** 442 (1992)
61. Modena A et al. *IEEE Trans. Plasma Sci.* **24** 289 (1996)
62. Mori W B et al. *Phys. Rev. Lett.* **72** 1482 (1994)
63. Lichtenberg A J, Lieberman M A *Regular and Stochastic Motion* (New York: Springer-Verlag, 1983)
64. Sheng Z-M et al. *Phys. Rev. Lett.* **88** 055004 (2002)
65. Sheng Z-M et al. *Phys. Rev. E* **69** 016407 (2004)
66. Malka G et al. *Phys. Rev. Lett.* **79** 2053 (1997)
67. Sarkisov G S et al. *Pis'ma Zh. Eksp. Teor. Fiz.* **66** 787 (1997) [*JETP Lett.* **66** 828 (1997)]
68. Delfin C et al. *Phys. Plasmas* **9** 937 (2002)
69. Rousseaux C et al. *Phys. Plasmas* **9** 4261 (2002)
70. Héron A et al. *Phys. Plasmas* **8** 1664 (2001)
71. Pukhov A, Meyer-ter-Vehn J *Phys. Rev. Lett.* **76** 3975 (1996)
72. Adam J C et al. *Phys. Rev. Lett.* **78** 4765 (1997)
73. Naumova N M et al. *Phys. Rev. E* **65** 045402 (2002)
74. Sentoku Y et al. *Phys. Rev. E* **65** 046408 (2002)
75. Weibel E S *Phys. Rev. Lett.* **2** 83 (1959)
76. Askar'yan G A et al. *Pis'ma Zh. Eksp. Teor. Fiz.* **60** 240 (1994) [*JETP Lett.* **60** 251 (1994)]
77. Gahn C et al. *Phys. Rev. Lett.* **83** 4772 (1999)
78. Meyer-ter-Vehn J, Sheng Z M *Phys. Plasmas* **6** 641 (1999)
79. Pukhov A, Meyer-ter-Vehn J *Phys. Rev. Lett.* **79** 2686 (1997)
80. Fuchs J et al. *Phys. Plasmas* **6** 2563 (1999)

81. Andreev A A et al. *Phys. Plasmas* **10** 220 (2003)
82. Lasinski B F et al. *Phys. Plasmas* **6** 2041 (1999)
83. Hatchett S P et al. *Phys. Plasmas* **7** 2076 (2000)
84. Tabak M et al. *Phys. Plasmas* **1** 1626 (1994)
85. Karch S et al. *Laser Part. Beams* **17** 565 (1999)
86. Cowan T E et al. *Nucl. Instrum. Meth. A* **455** 130 (2000)
87. Cowan T E et al. *Phys. Rev. Lett.* **84** 903 (2000)
88. Gahn C et al. *Appl. Phys. Lett.* **77** 2662 (2000)
89. Shkolnikov P L et al. *Appl. Phys. Lett.* **71** 3471 (1997)
90. Liang E P, Wilks S C, Tabak M *Phys. Rev. Lett.* **81** 4887 (1998)
91. Shen B, Meyer-ter-Vehn J *Phys. Rev. E* **65** 016405 (2002)
92. Fedoryuk M V *Asimptotika: Integraly i Ryady* (Asymptotics Integrals and Series) (Moscow: Nauka, 1987)
93. Pukhov A, Sheng Z-M, Meyer-ter-Vehn J *Phys. Plasmas* **6** 2847 (1999)
94. Tsytovich V N *Teoriya Turbulentnoi Plazmy* (Theory of Turbulent Plasma) (Moscow: Atomizdat, 1971) [Translated into English (New York: Consultants Bureau, 1977)]
95. Spencer I et al. *Phys. Rev. E* **67** 046402 (2003)
96. Maksimchuk A et al. *Phys. Rev. Lett.* **84** 4108 (2000)
97. Clark E L et al. *Phys. Rev. Lett.* **85** 1654 (2000)
98. Krushelnick K et al. *Phys. Plasmas* **7** 2055 (2000)
99. Mackinnon A J et al. *Phys. Rev. Lett.* **86** 1769 (2001)
100. Murakami Y et al. *Phys. Plasmas* **8** 4138 (2001)
101. Roth M et al. *Nucl. Instrum. Meth. A* **464** 201 (2001)
102. Andreev A A et al. *Zh. Eksp. Teor. Fiz.* **121** 266 (2002) [*JETP* **94** 222 (2002)]
103. Hegelich M et al. *Phys. Rev. Lett.* **89** 085002 (2002)
104. Mackinnon A J et al. *Phys. Rev. Lett.* **88** 215006 (2002)
105. Zepf M et al. *Phys. Rev. Lett.* **90** 064801 (2003)
106. Allen M et al. *Phys. Plasmas* **10** 3283 (2003); Habara H et al. *Phys. Plasmas* **10** 3712 (2003)
107. Kaluza M et al. *Phys. Rev. Lett.* **93** 045003 (2004)
108. Andreev A A et al. *Pis'ma Zh. Eksp. Teor. Fiz.* **79** 400 (2004) [*JETP Lett.* **79** 324 (2004)]
109. Okihara S et al. *Phys. Rev. E* **69** 026401 (2004)
110. Habara H et al. *Phys. Rev. E* **69** 036407 (2004)
111. Cowan T E et al. *Phys. Rev. Lett.* **92** 204801 (2004)
112. Allen M et al. *Phys. Rev. Lett.* **93** 265004 (2004)
113. Belyaev V S et al. *Pis'ma Zh. Eksp. Teor. Fiz.* **81** 753 (2005) [*JETP Lett.* **81** 616 (2005)]
114. Maksimchuk A et al. *Fiz. Plazmy* **30** 514 (2004) [*Plasma Phys. Rep.* **30** 473 (2004)]
115. Sentoku Y et al. *Phys. Rev. E* **62** 7271 (2000)
116. Bulanov S V et al. *Pis'ma Zh. Eksp. Teor. Fiz.* **71** 593 (2000) [*JETP Lett.* **71** 407 (2000)]
117. Ueshima Y, Sentoku Y, Kishimoto Y *Nucl. Instrum. Meth. A* **455** 181 (2000)
118. Lawson W S, Rambo P W, Larson D J *Phys. Plasmas* **4** 788 (1997)
119. Wilks S C et al. *Phys. Plasmas* **8** 542 (2001)
120. Pukhov A *Phys. Rev. Lett.* **86** 3562 (2001)
121. Zhidkov A et al. *Phys. Rev. Lett.* **89** 215002 (2002)
122. Esirkepov T Zh et al. *Phys. Rev. Lett.* **89** 175003 (2002)
123. Bulanov S V et al. *Fiz. Plazmy* **28** 1059 (2002) [*Plasma Phys. Rep.* **28** 975 (2002)]
124. Andreev A A, Litvinenko I A, Platonov K Yu *Zh. Eksp. Teor. Fiz.* **116** 1184 (1999) [*JETP* **89** 632 (1999)]
125. Sentoku Y et al. *Phys. Plasmas* **10** 2009 (2003)
126. Dong Q L et al. *Phys. Rev. E* **68** 026408 (2003)
127. Bulanov S V et al. *Fiz. Plazmy* **30** 21 (2004) [*Plasma Phys. Rep.* **30** 18 (2004)]
128. Silva L O et al. *Phys. Rev. Lett.* **92** 015002 (2004)
129. Roth M et al. *Phys. Rev. Lett.* **86** 436 (2001)
130. Bychenkov V Yu et al. *Fiz. Plazmy* **27** 1076 (2001) [*Plasma Phys. Rep.* **27** 1017 (2001)]
131. Geissel M et al. *Nucl. Instrum. Meth. A* **544** 55 (2005)
132. Borghesi M et al. *Phys. Rev. Lett.* **88** 135002 (2002)
133. Borghesi M et al. *Phys. Rev. Lett.* **92** 055003 (2004)
134. Patel P K et al. *Phys. Rev. Lett.* **91** 125004 (2003)
135. Mendonça J T, Davies J R, Eloy M *Meas. Sci. Technol.* **12** 1801 (2001)
136. Lancaster K L et al. *Phys. Plasmas* **11** 3404 (2004)
137. McKenna P et al. *Phys. Rev. Lett.* **91** 075006 (2003)
138. Bulanov S V et al. *Nucl. Instrum. Meth. A* **540** 25 (2005)
139. Gurevich A V, Meshcherkin A P *Zh. Eksp. Teor. Fiz.* **80** 1810 (1981) [*Sov. Phys. JETP* **53** 937 (1981)]
140. Kovalev V F, Bychenkov V Yu, Tikhonchuk V T *Pis'ma Zh. Eksp. Teor. Fiz.* **74** 12 (2001) [*JETP Lett.* **74** 10 (2001)]
141. Kosarev I N *Zh. Tekh. Fiz.* **75** (10) 73 (2005) [*Tech. Phys.* **50** 1323 (2005)]
142. Elkina N V, Levchenko V D *Voprosy At. Nauki Tekh. Ser. Mat. Modelirovanie Fiz. Protsessov* (4) 124 (2003)